EVOLUTIONARY BIOMASS CONVERSION IN PULP AND PAPER INDUSTRIES

REPORT 2018:534

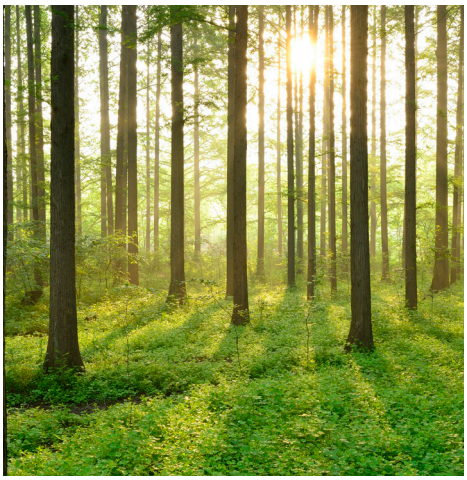

RESURS- OCH KLIMATEFFEKTIV SKOGSINDUSTRI

Energiforsk

Evolutionary biomass conversion in pulp & paper industries

Integration possibilities for a gasifier with an existing BFB combustor

OSCAR GRÜNDER, MARTIN SEEMANN

ISBN 978-91-7673-534-3 | © Energiforsk November 2018

Energiforsk AB | Phone: 08-677 25 30 | E-mail: kontakt@energiforsk.se | www.energiforsk.se

Foreword

Denna rapport är slutrapportering av projekt SE212 Termisk konvertering av restprodukter på pappersbruk inom forskningsprogrammet Resurs- och Klimateffektiv skogsindustri.

Programmets handlar i första hand om energieffektivisering och att kunna nyttiggöra såväl termisk som organiskt bunden energi i pappers- och massabrukens processströmmar. Projekt inom programmet ska ge lösningar på upplevda problem på bruken och ge möjlighet att använda forskningsresultaten kommersiellt inom en femårsperiod.

Projektet har haft som syfte att undersöka vilka gaskvalitéer man kan förvänta sig av olika restproduktsströmmar och med det som utgångspunkt föreslå olika processkonfigurationer och därmed visa den framtida utbyggnadspotentialen för massa- och pappersbruk.

Utförare har varit Chalmers med Martin Seeman som huvudprojektledare.

Projektet har följts av en referensgrupp bestående av:
Bertil Lundberg, Billerud Korsnäs
Kristian Elvemo, SCA
Johan Isaksson, Södra

Forskningen har möjliggjorts ekonomiskt genom medel från ÅForsk samt dessa bruk:

Billerud Korsnäs Frövi
Billerud Korsnäs Gävle
Billerud Korsnäs Gruvön
Billerud Korsnäs Karlsborg
Billerud Korsnäs Skärblacka
Munksjö Aspa
Rottneros Vallvik
SCA Munksund
SCA Obbola
SCA Östrand
Södra Cell Mönsterås
Södra Cell Mörrum
Södra Cell Värö

Samtliga bruk ovan har representanter i programstyrelsen.

Helena Sellerholm
Områdesansvarig
Termisk energiomvandling, Energiforsk AB

Sammanfattning

Förgasning av bark kan skapa ett energiflöde som kan göra bruk oberoende av fossila bränslen, men på medellång sikt är även produktionen av el eller syntesgas för framställning av kemikalier och bränslen tänkbart, beroende på vad brukets behov och marknadens efterfrågan är. Svårigheten är dock att göra rätt val i en osäker energimarknad där framtidens prissättning på både utsläppsrättigheter för koldioxid, kemikalier eller biobränslen är okänd, samtidigt som investeringar i förbrännings-/förgasningsanläggningar har behov av långsiktighet för att täcka sina kostnader. Under de förutsättningarna kan en indirekt påhängsförgasare som kan integreras med en befintlig fluidiserad bäddpanna av cirkulerande eller bubblande typ vara ett klokt val. Minst kapitalintensivt är att använda gasen som bränngas, dock kan förgasaren kombineras med en gasrening för användning mot högre renhetskrav. Eftersom pannan fortsatt kan köras som vanligt, dvs. utan förgasaren i drift, om inget behov för exempelvis bränngas finns är kopplingen till brukets övriga energiflöden mjuk och kan utvecklas efter hand.

Syfte

Projektet syftar till att undersöka vilka gaskvalitéer man kan förvänta sig från förgasning av bark och vilka processkonfigurationer som är intressanta. Specifikt undersöks experimentellt en koppling mellan två bubblande bäddar där sanden lyfts över ett bräddavlopp/fördämning mellan barkpannan och förgasaren med hjälp av riktad extra fluidisering. Som basfall för beräkningar och diskussioner används driftdata och dimensioner från BFB-pannan på Skärblacka bruk (BillerudKorsnäs) under en låglastperiod.

Bakgrund

Konceptet med en påhängsförgasare har demonstrerats på Chalmers i 2-4 MW skala sedan 2008 i över 25 000 drifttimmar, med stor tillförlitlighet. Tack vare integrationen med en befintlig anläggning och möjligheten att nyttja exempelvis dess styrsystem och annan infrastruktur har investeringskostnaden varit så låg som 13 MSEK för hela förgasaren. Till skillnad från Chalmersanläggningen där pannan är en så kallad cirkulerande fluidiserad bädd (CFB) är den vanliga panntypen på många bruk en bubblande fluidiserad bädd (BFB). Sanden i en BFB rör sig enbart inom bädden till skillnaden av en CFB där sanden transporteras ut i toppen av förbränningsrummet och återförs i botten av anläggningen. På så sätt finns en höjdskillnad som kan nyttjas i en CFB till att leda materialet genom en påhängsförgasare. Eftersom bäddmaterialens partikelstorlek, dp, i en BFB ligger över en millimeter, i jämförelse med CFB-material med dp mellan 0,2 och 0,5 mm, krävs det högre gashastighet att lyfta dessa partiklar. En annan aspekt är att momentet när en partikel kolliderar med en vägg, i framförallt cyklonen, ökar proportionellt med ~dp^3 och partikelns hastighet och bidrar således till en ökad nötning.

Koncept

Olika förslag hur en påhängsförgasare eller pyrolysreaktor skulle kunna kopplas till en BFB-panna, visas i Figur 1-3. Lösningen där man kopplar en CFB-förgasare/-pyrolysreaktor till en BFB-panna har demonstrerats i Joensuu, Finland (Figur 1). Bäddmaterial rinner ut genom ett snedrör till en riser där partiklarna transporteras upp

med hjälp av recirkulerade gaser och gaser som produceras under omvandlingen av bränslet som matas in i botten av pyrolysreaktorn. Partiklar separeras från gasen i en cyklon och återförs till pannan. Detta är en elegant lösning för att uppnå nödvändiga gashastigheter, men bränslematning in i en fluidiserad bädd är känslig och ovan nämnda erosionsproblem kvarstår.

De två andra lösningarna klarar sig utan riser och cyklon genom att man delar upp den bubblande bädden i två zoner som fluidiseras med ånga respektive luft. Figur 2 visar hur förgasaren och pannan delar den befintliga bädden genom att ångfluidiseringen når lite längre ut än förgasarens yta vilket säkerställer en luftfri atmosfär i denna. Gasatmosfären hålls separat med hjälp av en vägg som når ner under bäddens yta medans värmeöverföringen sker mellan partiklar och diffusion av partiklar tvärs under väggen. Denna lösning har undersökts i labbförsök som även visar att bränslets uppehållstid i själva förgasningsreaktor kan styras med hjälp av tryckbalansen mellan pannan och förgasare [13]. Genom att man minskar arean som fluidiseras med luft så minskar man även lägsta lasten som pannan kan köras sommartid då värmebehoven på bruken är mindre. Man minskar dock även högsta lastnivån, vilket man skulle kunna undvika genom att förse anläggningen med en möjlighet att elda gasen som produceras i förgasaren i antingen pannans fribord eller en separat gaseldad ångpanna. Om inte pannans area och lastområde kan förändras så kan man bygga till en förgasare vid sidan av pannan på liknande sätt.

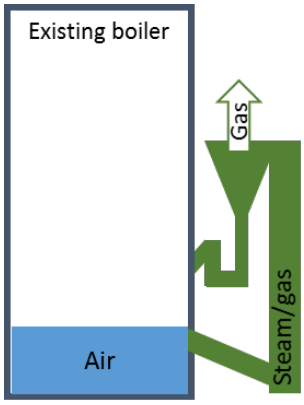

Figur 1: schematisk bild på en BFB/CFB combination

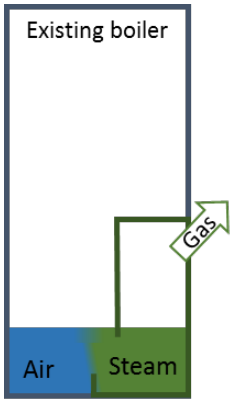

Figur 2: Värmeöverföring I bädden och separation genom olika fluidiseringsgaser

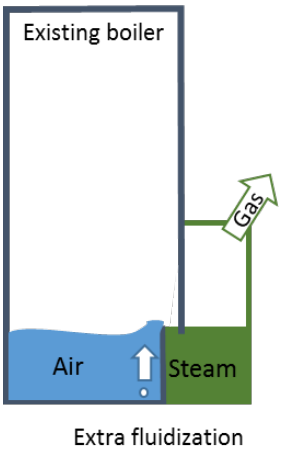

Figur 3: Lokal förstärkt fluidisering för materialtransport

En tredje möjlighet att flytta värme mellan två bubblande bäddar vilket visas schematiskt i figur 3 där bäddmaterialet lyfts i en zon med förstärkt fluidisering över en vägg eller breddavlopp. På andra sidan väggen är fluidiseringsgasen ånga och atmosfären hålls separat genom ytterligare en vägg som når ner en bit i bädden. Utloppet av förgasningsreaktorn är kopplat genom ett sandlås till pannans bädd och materialflödet drivs av den höjdskillnaden som den överförda sanden skapar. Eftersom den förstärkta fluidiseringen är en från panndriften oberoende parameter kan materialflödet styras och stängas efter behov.

Eftersom sambanden mellan förstärkt fluidisering och materialtransport över en vägg är okänd i motsatsen till de andra två koncepten är det den senare varianten som är

fokus i den experimentella undersökningen. Värmebalansberäkningar är dock giltiga för alla ovan nämnda fall.

Genomförandet

Projektet har genomförts i tre delar, insamling av tillgängliga data på barkförgasning i indirekta förgasningssystem, uppställning av energi- och värmebalanser samt en experimentell utvärdering av materialtransporten mellan två bubblande bäddar.

Resultat

Angående resultat för bark i industriella indirekta förgasningssystem har vi fokuserat på resultat från GoBiGas (32 MW_{th}) och Chalmersförgasaren (2 MW_{th}) eftersom data är framtagna på liknande sätt och därför är jämförbar. Detta är intressant med tanke på att det användes en olivinsand som har katalytiska effekter på GoBiGas medan resultat på Chalmers är framtagna med vanlig kiselsand som bädd. Det är påtaglig hur den katalytiska effekten påverkar utbytet av tjära vilka är oönskade biprodukter med aromatisk struktur. Koncentrationen av dessa är relevant om gasen ska kylas före användning då deras kondensationspunkter kan ligga så högt som 300 °C. Låga koncentrationer som i GoBiGasfallet är relativt oproblematiska vid nedkylning [39] medan de mängder som producerades med kiselsand kräver mer robusta åtgärder, som tvätt. Utöver olivinsand finns det andra material som visar liknande egenskaper, så som dolomit, kalksten eller fältspat.

Tabell 1: torr produktgassammansättning in vol-% *lätta kolväten är inkluderade som metan

Specie		Composition 20 % moisture	Composition 50 % moisture	GoBiGas [18] Olivine	Chalmers Silica sand
CO	Vol%	36,1	34,3	17-21	26,6
CO_2	Vol%	12,2	13,5	23-25	25,6
H_2	Vol%	35,1	35,9	39-43	30
CH_4	Vol%	15,6	15,4	7,1-8,7 (11,2*)	12,1 (16,5*)
tar	g/Nm^3			8-15	>50
LHV_{humid}	(MJ/kg)	8.36	5,6		
LHV_{dry}	(MJ/kg)	17,9	17,9	12,8	12,7

Energibalansen är framtagen med syftet att bestämma förgasarens värmebehov (heat demand) vilket ska täckas av pannan genom cirkulation av varm sand (Figur 4). Värmebehovet är summan av den latenta värmen i gasen, förångningsvärme för fukt i bränslet och reaktionsvärme för förgasnings- och pyrolysreaktioner. Eftersom varken uppehållstid eller temperaturen runt 800 °C är tillräckligt hög för full koksomvandling återförs en del av förgasarbränslet som koks tillsammans med bäddmaterialet till pannan (Qbed and char).

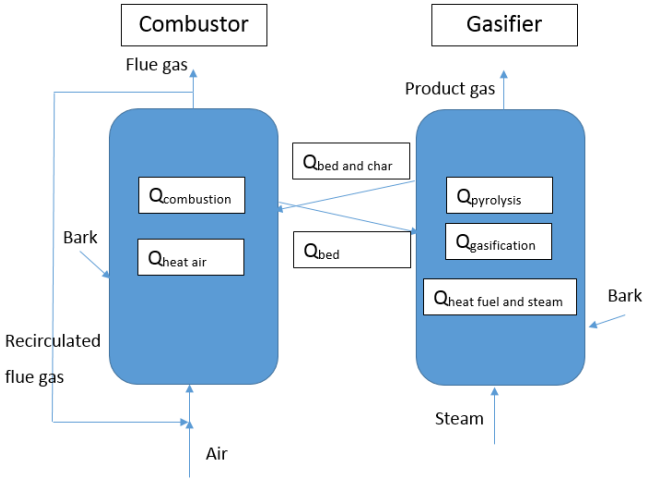

Figur 4: Schematisk bild av värmeflöden i ett kopplat fluidbäddsystem

Indata har baserats på barkpannan vid Skärblacka bruk (BillerudKorsnäs) för ett driftfall som producerar 30 t ånga/h, vilket motsvarar ungefär 20 MW baserat på lägre värmevärdet. Detta motsvarar driften under sommarmånaderna då pannan går på minlast.

Förgasarens storlek i termer av gasproduktione, baserat på lägre värmevärdet, och bränslets fukthalt har varierats mellan 4 och 18 MW respektive 0-50%. Minsta materialflödet mellan panna och förgasare för att täcka värmebehovet för varje fall har sedan beräknats. Som exempel visar figur 5 att materialflödet måste öka från 17 till 52 kg/s för en 12 MW förgasare vid ökande fukthalt.

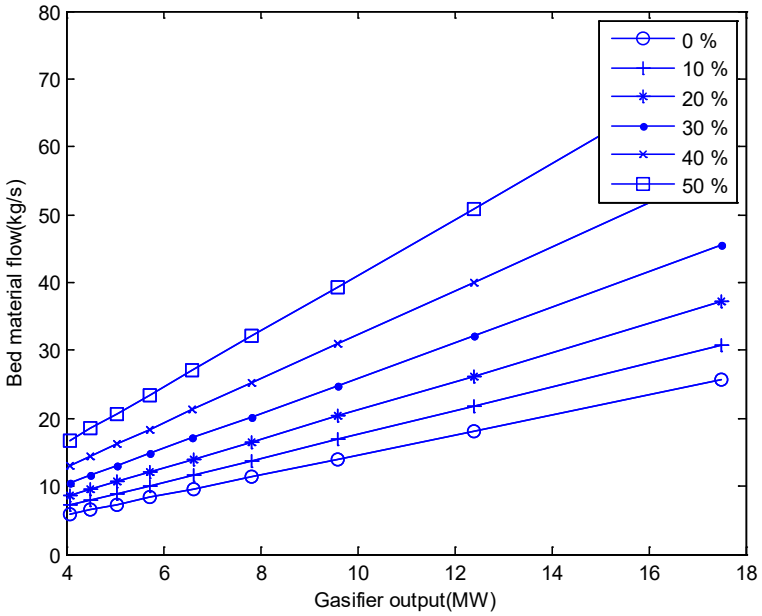

Figur 5: bäddmaterialflöde som krävs för att täcka värmebehovet av olika kombinationer av förgarastorlek och bränslefukt

För tre karakteristiska fall visas värmebehov och -fördelning i tabell 2. För icke torkad bark (50% fukt) visas två storlekar av förgasare, en på 17,5 MW_{gas} (Fall 1) och en på 9,7 MW_{gas} (Fall 2). Som jämförelse visas värmefördelningen för en 17,5 MW_{gas} förgasare och 20% fukthalt (Fall 3). Bortser man från eventuella begränsningar i cirkulationsflöde, visar fall 1 och 2 bästa balansen då koksens värmeinnehåll och förgasarens värmebehov nästan är i balans. Fall 2 och 3 representerar förgasare med ungefär likt stort värmebehov och således krav på bäddmaterialcirkulation, dock tillåter fallet med torkad bark en nästan dubbelt så stor gasproduktion. Dessa samband är av relevans om det finns en begränsning i hur mycket material och således värme som kan överföras mellan de två reaktorerna.

Tabell 2: Beräknat värmebehov och värmefördelning i systemet

		Förgasare Storlek, bränslefukt		
		17,5 MW 50%	**9,7 MW 50%**	**17,5 MW 20%**
Bränsle Input [MW]	Panna (LHV fuktig 50%)	-17,5	-21,4	-17,3
	Förgasare (LHV fuktig 20 or 50%)	-24,4	-13,2	-26,5
Värmebehov Förgasare [MW]	Uppvärmning torr gas (25-750 °C)	1,38	0,77	1,39
	Förångningsentalpi och uppvärmning (25-750 °C)	5,37	2,98	1,36
	Uppvärmning fluidiseringsånga (150-750 °C)	0,95	0,48	0,88
	Reaktionsvärme förgasning och vattengasreaktionen @750 °C	0,28	0,14	0,28
Värmetransport [MW]	Netto värmeöverföring genom bäddmaterial från förbränning till förgasaren ΔT=100 °C	8	4,6	4,3
	Koks från förgasning till förbränning	9	5	9,1
Förgasare output [MW]	Produktgas LHV	17,5	9,7	17,6
	Värme i produktgas Temperaturnivå 200 -25°C	7,72	4,2	3,63
Panna output [MW]	Producerad ånga	18,5	21,8	22,1
	Lågvärdig värme, under 100 °C	2,4	3	2,4

Mängden bäddmaterial som cirkulerar mellan pannan och förgasaren undersöktes med hjälp av nerskalade kallmodellsförsök. Vid sådana försök finns det enligt Glicksman vissa storheter och kvoter som ska hållas konstant för att garantera fluiddynamisk likhet.

I enlighet med konceptet skalades Skärblackapannan som är 8x8m i tvärsnitt ner till en 0,3x0,3 m plexiglasmodell. För att dessutom upprätthålla densitetsförhållandet mellan bäddmaterial och gas användes brons som bäddmaterial och luft som fluidiseringsgas (Figur 6). Väggen som begränsar utloppet slutade 2 cm över bäddens yta vid icke fluidisering, vilket motsvarar ungefär 0,5 m i barkpannan. Under utloppet över hela dess längd fanns möjligheten för tillförsel av extra fluidiseringsgas vilket resulterar i en kraftfull lokal fluidisering som lyfter en del av materialet över väggen (Figur 7).

Figur 6 Kallmodellen från topp med extra fluidisering

Figur 7 extra fluidisering från sidan

Den ovannämnda extra fluidiseringen varierades och utflödet av bäddmaterial mättes med hjälp av en våg. Materialflödet skalades sedan till barkpannans dimension per meter öppning och plottas mot flödet av extra fluidisering som motsvarar 0-13% av den ordinarie fluidiseringen genom primärluft och återförd rökgas (Figur 8). Gula markörer motsvarar standarduppsättningen medan andra kulörer är variationer av densamma. Det är tydligt att materialflödet ökar vid högre flöden av extra gas men även att spridningen av mätvärden ökar nämnvärd och att ”kurvan” planar ut. En ökad bäddhöjd (grön) vid samma avstånd till utloppets kant påverkar materialflödet negativt eftersom extragasen har tid att fördela sig över ett bredare område inom bädden och materialet kastas därför inte lika högt. Som förväntat resulterar en 50% ökad vägghöjd (röd) i en minskning av materialflödet. Att en halvering av utloppets bredd (blå) inte visar några större avvikelser per meter öppning bekräftar att öppningen kan förlängas eller kortas ner baserat på befintliga data.

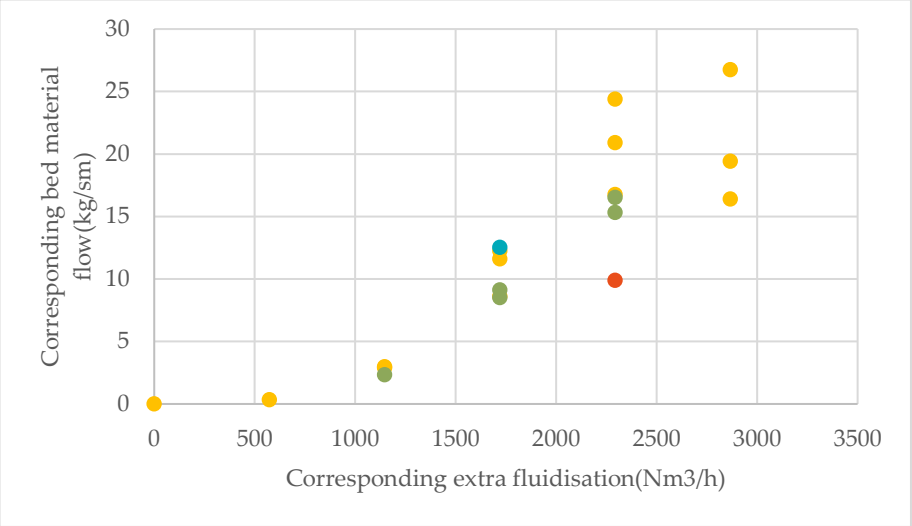

Figur 8: Bäddmaterialflöde per meter öppning för olika extra fluidisering omräknad till full skala, ●gul (referens) 1m hög bädd, ●blå 50% mindre öppning, ● röd 50 % högre vägg, ●grön 1.5 m hög bädd.

Sammanfattar man energibalansen och försökens resultat kan man definiera områden där systemet kan upprätthålla en designtemperatur på 850 °C i pannan. Med 10 % extra fluidisering uppnår man ett bäddmaterialflöde på cirka 20 kg/s per meter öppning, antar man vidare ett 2 m brett utlopp så visar den rödfärgade delen i Figur 9 möjliga förgasarstorlekar och bränslefukthalter. En förgasare som beräknades i fall 1 med en gasproduktion på 17,5 MW baserat på fuktig bark (50%) skulle kräva ett över 4 m brett utlopp eller ett orimligt högt bäddmaterialflöde per meter.

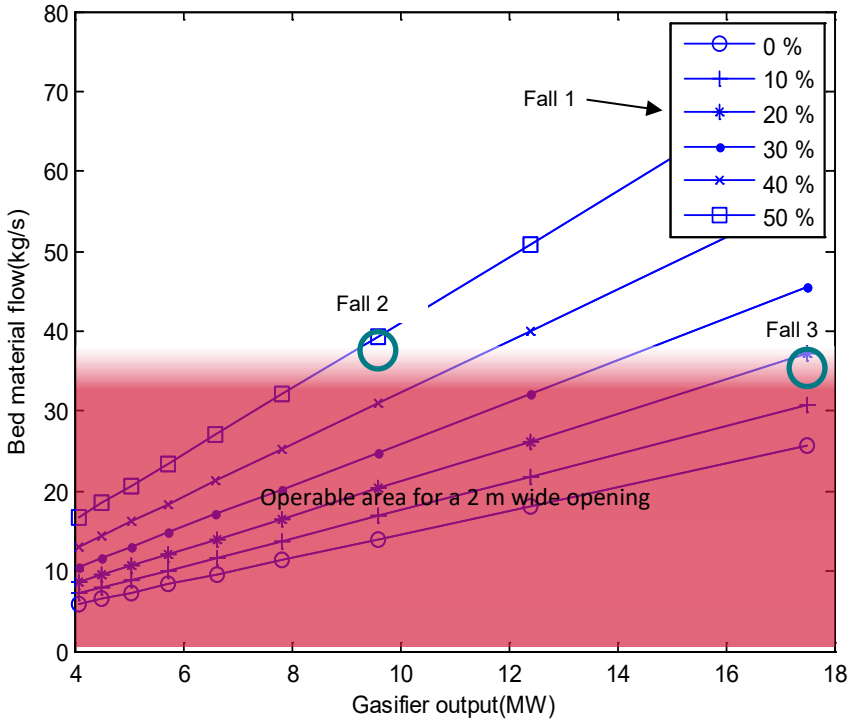

Figur 9: Bäddmaterialflöde som krävs för att täcka värmebehovet av olika kombinationer av förgasarstorlek och bränslefukt. Rödmarkerat område är realistiska fall vid ett materialflöde på 20 kg/s per m utlopp. Fall 1-3 motsvarar fallen i Tabell 2

Slutsatser

Inom projektet undersöktes möjligheten att komplettera en befintlig BFB-panna med en bubblande barkförgasare genom cirkulation av bäddmaterial som värmekälla till förgasningsprocessen. För att uppnå cirkulationen lyfts bäddmaterial lokalt med hjälp av extra fluidiseringsgas över en fördämning/vägg genom ett utlopp till förgasaren. Denna metod har undersökts i en nerskalad kallmodell som är fluiddynamiskt lik barkpannan på Skärblacka bruk (BillerudKorsnäs).

Resultaten visar att en cirkulation på 20 kg/s per meter öppning kan uppnås vilket är tillräcklig för att täcka värmebehovet från en förgasare med en gasproduktion mellan 9,7 och 17,5 MW_{gas} beroende på fukthalten i bränslet som varierades mellan 50 % och 20 %. Med tanke på tillgången till lågtemperaturvärme på bruket är det fördelaktigt att torka bark inför förgasningen för att kunna producera stora volymer gas med högt värmevärde (låg ånghalt).

De uppmätta cirkulationsflödena går att jämföra med ett cirkulationsflöde i en CFB-panna som vanligtvis ligger runt 1 kg/s per MW. För Skärblackafallet som är en 77 MW panna skulle det krävas att öppningen motsvarar cirka halva sidan av pannan för att uppnå 1kg/s och MW.

Rent allmänt har bark visat sig vara ett utmärkt bränsle i kombination med aktiva bäddmaterial eftersom specifika askämnen förstärker dessa effekter. Med den föreslagna tekniken kan bränngas med ett lägre värmevärde mellan 5 och 8 MJ/kg beräknad på fuktig bas produceras och via kondensering kan ett lägre värmevärde kring 13 MJ/kg uppnås.

Alla beräkningar är gjorda under förutsättning att barkpannan bibehåller samma ångproduktion som i basfallet, dock kommer integrationen med en förgasare inte lämna pannans drift helt opåverkad med tanke på värmemängden som extraheras med bäddmaterialet samt mängden koks som återförs till pannan från förgasaren. Eftersom koksen brinner huvudsakligen i bädden medan bark och dess innehåll av flyktiga komponenter i större utsträckning brinner ovanför bädden krävs högre primärluftflöde och mindre sekundärluft vilket leder till att mer värme kommer att frigöras i bädden. Under dessa förutsättningar kan det finnas potential att minska ångproduktionen under sommarmånaderna jämfört med nuläget, eftersom minsta fluidiseringshastighet lättare kan upprätthållas. Denna aspekt har dock inte legat i fokus för föreliggande utredning och kräver en djupare insyn i driftsförhållandena för Skärblackas panna.

Summary

This project has investigated the possibilities to add a gasifier onto an existing bark BFB combustor in pulp & paper plants by means of weir. The bark boiler of BillerudKorsnäs Skärblacka has been used as a reference plant, importing data and operating conditions from there. Investigation has been made on previous bark gasification plants, DFBG plants and bark composition papers giving reasonable predictions of resulting outputs of this retrofitted plant. Mass and energy balances have been established over this system in order to evaluate how much gas that can be produced, what quality the gas will have and how much energy is required in both combustor and gasifier to keep the energy balance in each chamber. The bed material transfer has been exclusively investigated in cold downscaled model experiments as well as an experimental of minimum fluidization velocity of the bed material at Skärblacka which have been compared with calculations made. The obtained bed material flow was compared with the heat and mass balance models in order to examine possibilities of implementation.

It has been discovered that the proposed setup of extra fluidization to the combustor can definitely provide a bed material flow high enough to reach the energy balance in the gasifier. The extra fluidization stream, which should constitute of recirculated gas, will require extra energy heating the gas, but will have only a small contribution on energy demands.

While the heat demand for the endothermic reactions of pyrolysis and gasification is relatively small in comparison the evaporation of moisture and the heating of the fluidization steam is to consider.

For the investigated cases a gasifier output almost as high as the combustor output is reachable for pre- dried fuel (20% moisture content?) in the gasification. Such dried fuel will also give a higher LHV of the product gas, which is favorable for all direct uses of product gas, e.g. in the lime kiln.

For higher moisture content the possible size decreases naturally as heat demand for evaporation of the moisture is dominating and will affect the heat balance in the furnace. Another effect on the operation of the boiler is the added amount of char from the gasifier which will likely affect the temperature distribution in the furnace as less volatiles are released. Simultaneous less secondary air is required as more fuel (char) is burning inside the bed which might allow to reduce the load of the boiler beyond the current level.

Those two effects should be investigated further as they could reduce unnecessary heat production during the warm periods of the year. With the investigations made in this project, it is a viable option to further investigate the installation of a gasifier onto the existing bark combustor with the suggested integration setup. The following conclusion can be drawn:

- Sufficient bed material can be transferred across a weir by means of directed extra fluidization to cover the heat demand of an 18 MW gasifier during low load operation of the BFB boiler
- Drying of the bark is recommended but even for moist bark a smaller sized gasifier can be realized with this concept.
- For further investigations the boiler operation should be included into the considerations.

Nomenclature

A	Area
D	depth
L	length
g	gravity
Re	Reynolds
u_{mf}	minimum fluidization velocity
u_t	Terminal velocity
dp	Particle diameter
m	Mass
n	mol
Q	heat
Cp	Heat capacity
M	Molar mass
x	Mass fraction
T	Temperature
V	Volume
p	pressure
ε	Void fraction
λ	Air to stoichiometric air ratio
ρ	density
τ	Residence time
μ	viscosity
ϕ	Sphericity
BFB	Bubbling fluidized bed
CFB	Circulating fluidized bed
DFB	Dual fluidized bed
DBFB	Dual bubbling fluidized bed
FG	Flue gas
·	flow

List of content

1 Background

1.1 INTRODUCTION AND AIM

This project was initialized by pulp & paper companies with a desire to make use for their bark residues in terms of gasification products instead of the current system which burn bark obtaining heat and power. Bark is the by-product in the pulp & paper industries debarking process, before the trees have been chipped and continue to the digester. The bark is utilized in a bubbling fluidized bed (BFB) combustor for steam production. However, the heat and electricity load varies significantly at pulp & paper industries between seasons. As a matter of fact, the energy content in bark is more useful during winter than during summer. To assure highest availablitiy of pulp and paper mills it is still desirable to run the bark combustor at minimum load even during summer in order keep a back-up heat production available that can be ramped up fast. The produced steam, however, is often not required at the site.

Gasification of the available bark volume would therefore be a better use of the bark if the gas can be used in the production process at site, replacing higher value fuels like propane, oil or tall oil. As gasification is an endothermic process a gasifier requires heat and can in principle efficiently be connected through the circulating bed material stream to a combustor forming an indirect gasification system. The advantage of such integration has been demonstrated for a 12MW_{th} CFB boiler situated at Chalmers. There, a 2-4MWth bubbling gasifier was integrated into the existing infrastructure utilizing the control system, steam and air grid. Due to those synergy effects the total investment was not more than 13 MSek. The gasifier has since 2008 operated for over 25,000 hours without mayor complications. The integration of the gasifier with a CFB-boiler is preferably between the down comer of the cyclone and the return leg providing naturally the height difference required for the bed material transport. For a BFB-boiler the integration is not self-evident as no directed bed material movement is assured.

This report investigates how a BFB gasifier can be attached to an already existing BFB combustor and how the bed material flows over a weir, separating the two volumes can be controlled. The bed material flow is experimentally investigated by cold downscaled experiments at Chalmers. A bark boiler at the site of BillerudKorsnäs in Skärblacka Sweden, is used as an example and operating conditions such as flows, temperatures, bed material characteristics and pressures at that plant are used to investigate how to integrate the BFB gasifier. This bed material flow is investigated in a downscaled model analyzing if the flow is high enough to transfer the necessary heat. Energy balances are made over the new system, including the heat transport of the bed material between the combustor and gasifier. The expected gas quality is based on available data from large scale experiments at Chalmers and GoBiGas.

1.2 BARK COMPOSITION

Before explaining conversion of bark, it has to be described what bark is constituted of, in comparison to the rest of the tree, the stem. The difference in composition between bark and stem provides somewhat different conversion characteristics.
The chemical composition of bark for different tree species is shown in Table 1. Bark is a lignocellulosic material mainly constituted of lignin, cellulose and hemicellulose extractives [1]. These components constitute of carbon, oxygen and hydrogen but there

is also inorganic components, or minerals, in bark. The inorganic content is around 0.5 % in stem and 2-3 % in bark [2]. As seen in the table, the composition alters a lot between the tree types where the softwoods have a significantly higher cellulose content than the hardwood. However, the extractives content in bark is high in all cases compared to the stem wood, where the extractives content is about 2-5 % [1]. The extractives differ between hardwoods and softwoods. In hardwood outer bark, a very common extractive is suberin [3].

Table 1: Main chemical compounds in stem and bark in different trees common in the Nordic countries (dry weight %) [1]

Type of tree	Type	Cellulose	Hemicellulose	Lignin	Extractives
Scots pine	Stem	40.7	26.9	27.0	5.0
	Bark	22.2	8.1	13.1	25.2
Norway spruce	Stem	42.0	27.3	27.4	2.0
	Bark	26.6	9.2	11.8	32.1
Silver birch	Stem	43.9	28.9	20.2	3.8
	Bark	10.7	11.2	14.7	25.6

In pulp and paper plants, the bark is often removed from the stem together with water, giving it a high moisture content. The moisture content can be as high as 50 % if no drying is made. The pulp mill at Värö, Sweden used to dry its bark to 10 % moisture content prior gasification in the now shut down air blown gasifier and in Joutseno, Finland, the bark is dried to 15 % [4] [5]. Drying is achieved with a belt dryer. Further drying may increase costs on a level where it becomes inefficient investments. The moisture content of interest is therefore in the range of 10-50 %.

Bark as most solid fuels consists of char, volatiles and ash, which characterize the thermal conversion the fuel undergoes in a gasification. After drying of the remaining moisture of the fuel inside the gasifier, volatiles are released in a temperature range 200-550 °C. in case of pyrolysis the conversion process is interrupted there and char, consisting mostly of carbon, remains. In case of gasification, at least a part of the char is gasified by means of a steam or carbon dioxide atmosphere into carbon monoxide and hydrogen, while the rest is combusted to balance the heat demand of this endothermic reaction. In an indirect gasification or pyrolysis process the char is commonly combusted in the adjacent boiler. If char can be used elsewhere, separation of char would be an option.

The composition of bark has been thoroughly tested and the average composition is presented in Table 2 [6]. In this project, it is assumed that char only consists of carbon.

Table 2: Average content of bark, expressed as in energy terms

Component	Share (w-%)
Volatiles	74.23
Char	22.63
Ash	3.13

The volatile specie composition estimation is made using LHV values from literature. The LHV of bark has been measured and the resulting average value is 20.28 MJ/kg dry ash free (daf) fuel [6] [7].

1.3 THERMOCHEMICAL CONVERSION OF BARK

As mentioned earlier, the thermochemical conversion of bark can be described by drying, pyrolysis, combustion and gasification. To obtain a gas with high calorific value the gasifier is preferably fluidized with steam to prevent dilution with nitrogen.
. Table 1 shows only the dry content of stem and bark, but in reality, the moisture content can be anything between 30-50 weight-% of harvested biomass [2]. The moisture content of bark can exceed this number depending on the storage and the weather conditions. The evaporation of water is strongly endothermic with a heat demand of 2.4 $MJ/kg_{evaporated}$. As the evaporation of the fuel humidity is the dominating heat sink in the gasification reactor drying of the bark is beneficial for the process.

Pyrolysis is the thermochemical conversion step where the volatile compounds get released at temperatures between 200-550 °C when bark is heated in absence of oxygen [2]. By pyrolysis of bark, mainly products are formed according to the total reaction (Eq 1), which is slightly exothermic. The reaction presented here is not balanced and the fraction of the products varies depending on operating conditions. $C_xH_yO_z$ represent hydrocarbons, oxygenated to different degrees. With increasing temperature those species are further converted and the oxygen content decreases. Hydrocarbons formed in this process are partially condensable already at temperatures below 300 °C and consist mainly of poly aromatic species usually labeled as tar.

$$C_nH_mO_p \rightarrow CO + CO_2 + CH_4 + C_xH_yO_z + H_2O + H_2 + C \qquad \text{Eq(1)}$$

The conversion of the remaining char (C), through the gasification reaction, is a slow reaction at the typical temperatures in an indirect gasifier (800-850 °C). The gasification reactions are shown in Equation 2. These reactions are endothermic and demand heating in order to maintain a constant gasification temperature, which should be around 800-1000 °C [2]. As seen, gasification is when a solid fuel is converted into combustible products like CO and H_2 [8].

$$C + CO_2 \rightarrow 2CO \qquad \text{Eq(2a)}$$
$$C + H_2O \rightarrow CO + H_2 \qquad \text{Eq(2b)}$$

As a matter of fact, the majority of the char is following the bed material into the combustion BFB and is combusted.

Combustion takes place when bark is heated and oxygen is present. The simplified overall reaction of biomass combustion is shown in Equation 3 [2]. In reality, numerous of radical reactions occur, oxidizing the biomass more and more until only CO_2 and H_2O is present, making the fuel fully oxidized. An important combustion reaction is the one of char, shown in Equation 4. The temperature needs to be above 600 °C for combustion to take place and as long as there is oxygen available, the reactions are fast.

$$C_xH_yO_z + \left(x + \frac{y}{4} - \frac{z}{2}\right) O_2 \rightarrow xCO_2 + \frac{y}{2}H_2O \qquad \text{Eq(3)}$$
$$C + O_2 \rightarrow CO_2 \qquad \text{Eq(4)}$$

Dual fluidized bed reactors have been used in many industrial applications and the addition of a gasifier to a CFB has been demonstrated successfully at Chalmers with more than 25000 hours of operation, however the concept of dual bubbling fluidized bed (DBFB) reactors is less tested.

In Figure 1 a schematic overview of a DBFB system is shown. The combustor is fluidized with air and recirculated flue gas and the gasifier is fluidized with steam. This prevents presence of N_2 in the gasifier. In the combustor energy is released by oxidation reactions and that energy is required to heat the fuel, fluidization stream and the bed material coming from the gasifier. The gasifier obtains heat from the bed material from the combustor, which is required to heat the fuel and steam as well to compensate for the endothermic pyrolysis and gasification reactions, keeping temperature constant in the gasifier. Char not gasified in the gasifier will follow the bed material into the combustor where it will be combusted. The amount of gasified char is mainly dependent on temperature and residence time in the gasifier.

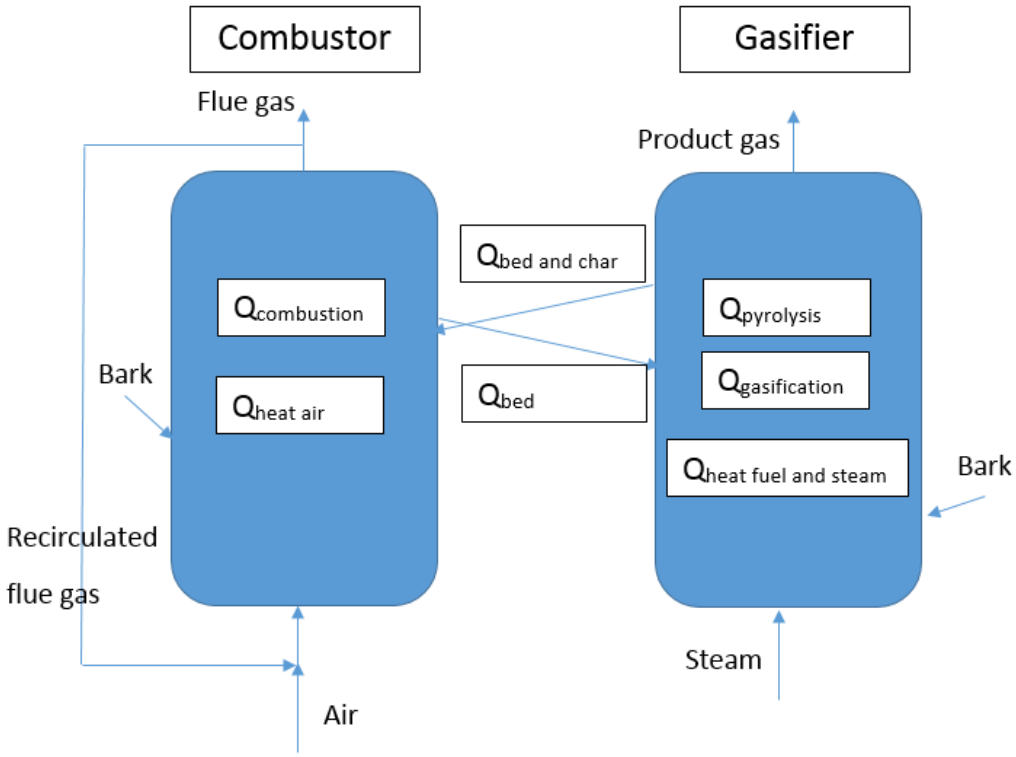

Figure 1: Overview of a DBFB system

Bubbling fluidized bed reactors have been used for both combustion and gasification in many plants with different fuels. The bed material is usually made of different sand materials depending on which characteristics are desired. It is in some applications wanted to have bed material that can carry oxygen from one reactor to another, where ilmenite have been proven to be an effective material [9]. In indirect gasification olivine an iron-magnesium-silicate mineral has been employed at GoBiGas and elsewhere for its ability to reduce the tar yield [10]. In this project no specific bed material has been considered, however the properties of regular silica sand has been used for calculations.

1.4 POSSIBLE INTEGRATION OPTIONS

The more common way to implement dual fluidized beds with combustion and gasification is to have at least one circulating fluidized bed, a CFB. It has been suggested that the most efficient choice is to have gasification in a BFB and combustion in a CFB [11].

Dual BFBs is not common in industrial applications due to limitations in the heat transfer due to a limited bed material circulation. Suggested setups employ two BFBs where a riser is attached to the top of the gasification BFB where solids and gas are separated with a cyclone making the solids return to the combustion BFB [12]. The fluidization agent has to be inserted by a so called minimum fluidization velocity, u_{mf}, a velocity which lifts the population of particles creating fluidization. BFBs are often operating with a superficial velocity several magnitudes above the minimum fluidization velocity without entrainment of large amounts of particles. u_{mf} is dependent on the fluidizing agent and bed material properties and is discussed in detail in Section 3.1.

For a riser, however, particles need to be transported upwards which requires an even higher superficial velocity, the so called terminal velocity, u_t. The commonly used larger diameter of the bed material particles (dp) in BFB reactors requires high gas flow rates to transport those particles. As a matter of fact, this implies even extreme stress and wear on the construction materials in a riser due to the higher momentum, which is proportional to ~dp^3 and the velocity. The reason for the larger dp in a BFB combustor is the desire to reach high fuel loads per meter square of the combustion bed. Consequently, larger particles withstand higher gas velocities without being entrained and allow for higher fuel load considering a given cross section.

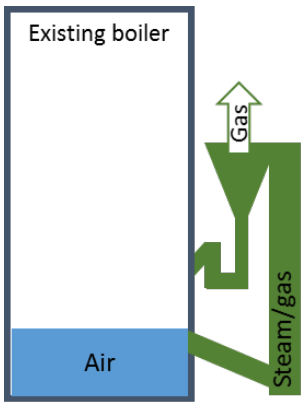

Figure 2: Simplified DBFB system, Riser/CFB, example Joensuu

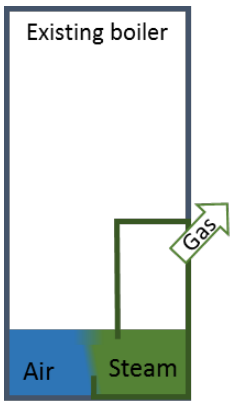

Figure 3: Setup of a DBFB system. Heat transfer in the bed, separation by fluidization

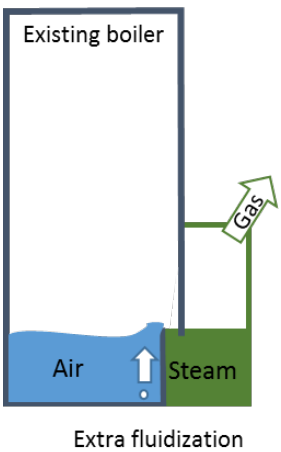

Figure 4: Simplified DBFB system evaluated in this project. emphasized flow by directed fluidization

At Joensuu, Finland, a pyrolyser coupled to a combustion unit is constructed according to this principle and simplified scheme is shown in Figure 2. The pyrolyser is a riser where gases, char and bed material rises to a cyclone where solids are separated from gases. The solids enter the combustor where the char is burned. Since the residence time in the pyrolyser is just a few seconds and the temperature is around 500 °C, no gasification reactions happen. By utilizing the pyrolysis gases produced from the fuel as additional driving force, contributing to u_t, enough bed material can be transferred making the energy balance easy to reach. However, above mentioned erosion issues remain.

To overcome erosion issues, while still reaching the required heat transfer between the beds, two theoretical DBFB configurations excluding risers and cyclones have been suggested.

The configuration in Figure 3 shows a combustor and gasifier sharing the same bed while comprising separated atmospheres. The chambers are only separated by a vault which ends below the surface of the fluidized bed. If designed correctly, no air will flow to the gasifier but some steam will flow to the combustor. The bed material and more importantly heat on the other hand will transfer between gasifier and combustor by convective transport and inter-particle heat transfer. Cold flow experiments of such a configuration have been investigated and have shown promising results [13]. Currently, further development of option is currently done in a project funded by Energimyndigheten and was therefore not included into the focus of this work.

The setup which has been chosen to investigate further in this project is shown in Figure 4. Here, the bed height is slightly lower in the combustor, but extra fluidization at the outlet makes bed material transfer from the combustor to the gasifier. The bed material will naturally flow back to the combustor since its level is higher at another outlet. The more extra fluidization at the combustor outlet will increase bed material transfer, but the disadvantage with increased flow is that more fluidization media is required and therefore the energy balance more difficult to reach. In this setup the openings between the reactors are at the gas part of the chambers and it is therefore more likely that air flows into the gasifier and steam into the combustor. It may therefore be convenient to place a seal between the beds. One expected challenge with this setup is the desired bed material transfer to reach the energy balance.

1.5 EXPECTED COMPOSITION OF PRODUCT GAS

In Table 3 gas qualities from the gasifier in different experiments are shown. All examples are taken from plants with dual fluidized bed gasification units where most units have a BFB gasifier and CFB boiler, the exception is [14] which has the opposite, [15] has two CFBs and [12] has 2 BFBs with a riser. All plants run with steam as fluidizing agent in the gasifier. Parameters such as bed material, residence time, pressure, gas velocity, steam/fuel ratio and possible post DFBG operations are different for these plants and is the reason for the varied results. The table shows however that both the CO and H_2 concentration varies between 15 and 50 %, when one is high the other is low and that is probably due to different steam/fuel ratios, affecting the WGS reaction. The CO_2 content varies between 10 and 28 and the CH_4 between 7 and 18. Most of the temperatures in the gasifier are kept between 800 and 850 °C but there is no clear relation between gas composition and temperature. Observing the average values,

the CO and H_2 content is in similar magnitude where CO_2 is lower and CH_4 even lower.

Table 3: Main gas compositions (dry vol-%) and temperature °C) in the gasifier in experiments gasifying biomass, mostly woody biomass. The remaining components are mainly N_2 and tars

Plant	CO (w-%)	H2 (w-%)	CO2 (w-%)	CH4 (w-%)	T_{gas} (°C)	Fuel
ECN(2004) [16]	28.0	23.0	28.2	9.11	850	Wood
ECN(2014) [17]	26.3	16.9	18.8	18.3	?	Biomass/waste
GoBiGas [18]	17-21	39-43	23-25	7.1-8.7	850	Bark
Güssing [19]	20-30	35.45	15-25	8-12	900	Wood chips
Milena(2009) [14]	37-39	18-20	11-13	14	850	Dry wood
Chalmers [20]	33.1	25.1	14.8	11.8	825	Wood pellets
Chalmers	26.6	30	25.6	12.1	820	Bark
SilvaGas [15]	50	15	10	15	?	Biomass
CAPE FICFB [21]	28.4	21.7	17.4	11.6	753	Wood pellets
HOULE-MCF [22]	25.1	33.1	19.3	10.4	?	?
Blue Tower [23]	15	50	25	10	950	Wood pellets
Yokohama [24]	29.2	31.2	17.3	13.7	820	Coffee grounds
NIAST [12]	26/29	40/34	28/23	9/9	800	Oak Sawdust
ECCMB [25]	26-30	40-44	16.23	9-13	800	Pine sawdust
Average	29.8	30.8	18.3	11.7	832	-

1.6 IMPLEMENTATION POSSIBILITIES IN PULP & PAPER INDUSTRIES

The requirements on the gas produced from the gasifier will heavily depend on the application the gas will be used for. Principally two areas for application are of interest, drying of paper either by heating of air or flue gas and the usage in the lime kiln.

In the lime kiln the calciumoxid used for the chemical recovery reactions creating white liquor out of green liquor is regenerated. In the calcination step, $CaCO_3$ is oxidized into CaO, according to Equation 9. The $CaCO_3$ enters on the opposite side of the fuel and air, where it gets dried. As the $CaCO_3$ gets further into the reactor it heats up and eventually oxidizes into CaO.

$$CaCO_3 \rightarrow CaO + CO_2 \qquad \text{Eq(9)}$$

Often fuel oil, commonly of fossil origin, is used in lime kilns. Implementing gasified bark will both decrease the use of fossil fuels and reduce fuel cost for the lime kiln, since estimated bark cost is 6-8 €/MWh and fuel oil is 25-30 €/MWh in Scandinavia [31]. Lime kiln capacity can be restricted since larger gas flow is needed and therefore the end temperature of the kiln increased. The lime quality can also be affected since some inorganic elements may follow the gasification flow. Previous implementation of wood residue gasification for lime kiln fuel has shown to change colour of the lime but not the quality [31]. The LHV for the gasified bark is around 5-7 MJ/kg at Joutenso which thereby is an approved gas quality to power the lime kiln [31].

1.7 PURIFICATION METHODS

Depending on the utilization an issue with gasification is the gas purification needed [27]. The required gas quality, however, depends on the demands of the downstream

equipment which lies beyond the scope of this project. To give some indications examples for different levels of complexity are presented below.

If the gas is to be used in the lime kiln no cleaning is required if the gas can be held above 300 °C and if fly ash particles are acceptable. For higher quality usage filtration of the gas is essential, furthermore, tar and steam condensation and removal is preferable if the gas should be transported over longer distances.

The particulate removal can be made with cyclones, ceramic or bag filters, electrostatic filters or solvent scrubbers [32]. Cyclones, however they cannot remove smaller particles than 1 μm [33]. Barrier filters can remove particles down to 0.5 μm and can handle high temperatures depending on what material it is made of. Ceramic fiber filters can operate at temperatures up to 900 °C which makes it even possible for the filter to be placed right after the gasifier before cooling the gas [33]. To assure alkali removal the filter temperature is preferably below the condensation temperature of alkali salts and rather in the range of 200-350 °C.

Tars are a term for hydrocarbons formed during the thermal conversion and comprise a mix of numerous organic compounds mostly of aromatic and polyaromatic nature. Common tars are benzene, toluene, naphthalene and phenanthrene [31]. Tar removal should be adapted to the utilization of the gas. While a high grade of purity (ppm levels) is required for synthesis processes such like methanol synthesis or Fisher-Tropsch synthesis, combustion in a burner or and engine requires only removal of the condensing species.

Tar can be removed by cracking/reforming [32] where even CH_4 and C_2 -hydrocarbons are cracked to syngas [16]. However, the most common way of removing tars is with scrubber columns. Tars can be removed by water quenching from a spray tower, separating the condensed tar from the rest of the gas. GoBiGas, for example, uses RME (rapeseed methyl ether) as scrubbing agent [35] for the condensable tar and absorber beds for the light tars, such like benzene. The light tars and scrubber liquid get separated in a stripper run by air/steam and is returned to the gasifier.

A special scrubbing solution is OLGA a two-stage scrubbing process which is more complex as it comprises stripper columns for regeneration of the scrubbing liquids [34]. The OLGA process has been demonstrated in different demonstration plants, achieving almost full removal of tars [16].

For the utilization as fuel in a burner most likely condensation of steam and tar in a heat exchanger is sufficient. A method recently demonstrated with surface modified plate heat exchangers provided by AlfaLaval [36] which simplifies the process layout drastically.

2 Modelling of a DBFB system

2.1 HEAT AND MASS BALANCES OF A DFBG SYSTEM

Heat and mass balances were created to assess the heat transfer between the beds in a DFBG system and to take forward parameters that describe the operation based on thermodynamic limitations. This model is a description of a DBFB configuration based on the bark boiler at the Skärblacka paper mill.

A mass balance inside the gasifier is made shown in Equation 14 where fuel (bark), steam and recirculated bed material from the combustor enters the gasifier where the gases leaves the gasifier in a product gas stream and the solids are recirculated back to the combustor. Steady state is assumed and $\dot{m}_{bed,c} = \dot{m}_{bed,g}$, so that there is always the same amount of bed material in the beds. The char that goes to the combustor will be oxidized and the gasification products, volatiles and steam will leave in the product gas.

$$\dot{m}_{steam}+\dot{m}_{bark,g} + \dot{m}_{bed,c} = \dot{m}_{PG} + \dot{m}_{bed,g} + \dot{m}_{char,c} \quad \text{Eq(14)}$$

A mass balance inside the combustor is shown in Equation 15. The fluidization inlet is a mix of recirculated flue gas and air. Depending on the load of the two reactors different shares of char from the gasifier and bark is combusted to CO_2 and H_2O and leaves as flue gas. As mentioned earlier, the bed material transfer is accordingly $\dot{m}_{bed,c} = \dot{m}_{bed,g}$.

$$\dot{m}_{combfluid} + \dot{m}_{bark,c} + \dot{m}_{bed,g} + \dot{m}_{char,c} = \dot{m}_{FG} + \dot{m}_{bed,c} \quad \text{Eq(15)}$$

The bark is assumed to only consist of C, H, O, ash and moisture. The ash is assumed to be inert. The dry ash free fuel is then divided into char and volatile species. The char is assumed to only consist of C, meaning that the total amount of C, H and O in volatiles is known from the ultimate analysis. However, which molecules that gets released as the volatiles is unknown and is modelled using some simplifications.

The heat balance of the gasifier shown in Equation 16 is calculated so the net energy of incoming and reacting entities is 0. The temperature in the gasifier was chosen to be 750 °C and 850 °C in the combustor and the temperature is constant in both reactors. The excess heat in the combustor is assumed to be taken up by steam and water in the heat exchanger surfaces inside the boiler. The steam to the gasifier is assumed to enter at 150 °C and the fuel at 25 °C. It is assumed that all incoming species are heated up to the temperature of the reactor and then reacted to other compounds. The reactions that take place in the gasifier are the WGS reaction, Equation (6) and the gasification reaction, Equation (4b).

$$\dot{Q}_{steam} + \dot{Q}_{fuel,gasifier} + \dot{Q}_{reactions,gasifier} = \dot{Q}_{bed\ material\ from\ combustor} \quad \text{Eq(16)}$$

The heat balance in the combustor is presented in Equation 17. The combustion refers to the combustion of char and some volatiles. The fuel enters at 25 °C and the fluidizing agent between 25 and 200 °C, see Section 2.2.

$$\dot{Q}_{Fluidizing\ agent} + \dot{Q}_{fuel,combustor} + \dot{Q}_{bed\ material\ from\ gasifier} = \dot{Q}_{combustion} \quad \text{Eq(17)}$$

The model is balanced that the required energy flow from the bed material to the gasifier is as large as the energy demand in the gasifier. That will give a required bed material flow between the beds which, corresponds to the required heat transfer.

One must keep in mind that the mass flow of bed material from and to the reactors is equal so no change in bed height over time occurs.

The heat demand for every specie is calculated as in Equation 18, in which c_P is integrated over the temperature rage and where i can be any compound. C_P-values are imported from NIST Chemistry Webbook.

$$\dot{Q}_i = \dot{n}_i \left(C_{P,A}(T_{reactor} - T_{inlet}) + \frac{C_{P,B}\left(T_{reactor}^2 - T_{inlet}^2\right)}{2} \right) \quad \text{Eq(18)}$$

The fluidizing agent to the gasifier is steam where a steam to fuel (SFR) ratio is used which can be described as the inlet mass flow of fluidizing steam divided by the inlet mass flow of dry fuel into the gasifier. The lower the SFR the less energy is required to heat the steam, but too low steam flow and the bed will not fluidize properly. A SFR of 0.5 has been used in all modelling cases, based on previous DFBG evaluations [41] and experiences from optimizations. The dry gasifier mass flow will be altered in the modelling, explained in Section 2.4, and therefore the steam flow. To keep the superficial gas velocity constant the bottom area of the gasifier is corrected to the steam flow, to always guarantee good fluidization.

2.2 FLUIDIZING AGENT OF THE COMBUSTOR

The inlet volumetric flow of fluidizing agent into the combustor is made of air and recirculated gas from the outlet of the combustor, shown in Figure 5.

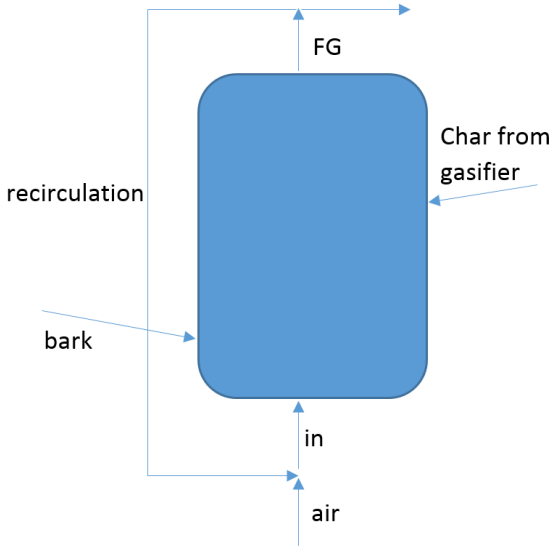

Figure 5: A simplified system for the entering gas, flue gas, fuel feed and recirculation for the combustor.

Air is assumed to constitute of 23.3 % O_2 and 76.7 % N_2 on a mass basis. The recirculated gas is assumed to be constituted of N_2, O_2, H_2O and CO_2 recirculated at 200 °C. The overall balance of the inlet of fluidizing agent is expressed in Equation 19.

$$V_{in} = V_{air} + V_{recirculated} \quad \text{Eq(19)}$$

where

$$V_{air} = \frac{m_{O_2,air}}{\rho_{O_2,25°C}} + \frac{m_{N_2,air}}{\rho_{N_2,25°C}}$$

$$V_{recirculated} = \frac{m_{O_2,recirculated}}{\rho_{O_2,200°C}} + \frac{m_{N_2,recirculated}}{\rho_{N_2,200°C}} + \frac{m_{CO_2 recirculated}}{\rho_{CO_2,200°C}} + \frac{m_{H_2O,recirculated}}{\rho_{H_2O,200°C}}$$

For this calculation, it is assumed that all fuel is converted to CO_2 and H_2O according to how much C and H the inlet fuel contains. As the amount of air to the reference combustor at low load was given the amount of fuel put into the combustor was adjusted to give the system an air-to-fuel ratio (λ-value) of 1.2. The air-to-fuel ratio is explained in Equation 20.

$$\lambda = \frac{\dot{n}_{O_2,in}}{\dot{n}_{O_2 teoretical}}$$

where

$$\dot{n}_{O_2 teoretical} = \frac{\dot{n}_{CO,pyr}}{2} + \frac{\dot{n}_{H_2,pyr}}{2} + \frac{4\dot{n}_{CH_4,pyr}}{2} + \frac{15\dot{n}_{C_6H_6,pyr}}{2} + \dot{n}_{char} + \dot{n}_{char\ from\ gasifier}$$

Eq(20)

The combustible fuel is the sum of the char from the gasifier, char from the fuel bark and CO, H_2, CH_4 and tar from the volatiles in the bark. That will also give how much CO_2 and H_2O is produced during combustion respectively. However, the distribution of bark fed to the combustor and char coming from the gasifier is a parameter that is desired to be varied during the modelling.

A factor between molar flow of char from the combustor fuel and molar flow of char from the gasifier entering the combustor was introduced. The molar flow of char from the combustor fuel is constant, meaning that with varying factors, the fuel flow from the gasifier will change.

The composition of the recycled gas will be the same as in flue gas and the amount is adjusted in order to reach the set volumetric flow required for fluidization. Based on that the inlet fractions of the total fluidization mass flow are known.

The expression for all inlet flows are shown in Equation 21 with x representing the share of flue gas recirculated and y_{CO2} is the share of combusted fuel forming CO_2, based on C and H content in the fuel. y_{CO2} is around 61 % since there is also a char addition from the gasifier. The H_2O content comes both from combustion, but also from moisture content. The contribution from the moisture content makes the expression a bit more complicated, but that is necessary in order to have it expressed as inlet oxygen flow from the air stream since that is a known amount. The gasifier factor is the fuel ratio between the combustor and the gasifier and is used to vary the size of the gasifier, since the size of the combustor is set by the air flow.

$$n_{N_2,in} = n_{N_2,air}\left(1+\frac{x}{1-x}\right)$$

$$n_{O_2,in} = n_{O_2,air}\left(1+\frac{x(\lambda-1)}{1-x\lambda+\mathrm{x}}\right)$$

$$n_{CO_2,in} = n_{O_2,air}\frac{xy_{CO2}}{\lambda(1-\mathrm{x})}\left(1+\frac{x(\lambda-1)}{1-x\lambda+\mathrm{x}}\right)$$

$$n_{H_2O,in} = n_{O_2,air}\left(1+\frac{x(\lambda-1)}{1-x\lambda+\mathrm{x}}\right)\left(\frac{x_H}{2M_H}+\frac{x_{mois}}{M_{H_2O}(1-x_{mois})}\right)\frac{xM_C}{(1-x)\lambda x_C\left(\frac{M_C x_{combshare} x_{vols}}{M_{comb} x_C}+1+\frac{1}{gasifierfactor}\right)}$$

Eq(21)

The molar flows are translated to mass flows, shown in Table 5 for a case with a gasifier factor of 1.0. Due to a moisture content as high as 50 %, the recirculated stream contains much more H_2O than CO_2.

Table 4: Mass flow rates combustion fluidization inlet

Specie	Mass flow (kg/s)	Mass flow air (kg/s)	Mass flow in (kg/s)
N_2	1.666	2.775	4.441
O_2	0.068	0.843	0.911
CO_2	0.269	0	0.269
H_2O	0.321	0	0.321

2.3 PYROLYSIS CONTENT

In reality pyrolysis gases released from the fuel in the gasifier contain numerous types of hydrocarbons but is represented in the calculations by CO, H_2, CO_2, H_2O, CH_4 and C_6H_6, a simplification of Equation 1. Light hydrocarbons are represented by CH_4 and heavy hydrocarbons by C_6H_6.

The LHV for the product gases is calculated as in Equation 22. The units of LHV_{bark} and LHV_{dev} are MJ/kg daf fuel whereas LHV_{char} is MJ/kg char. The resulting unit for LHV_{pyro} is MJ/kg volatiles. x_{char} and x_{vols} are given as present of daf fuel. The calculated LHV_{pyro} is 16.13 MJ/kg volatiles which is higher than the corresponding value for the humid bark.

$$LHV_{pyro} = \frac{LHV_{bark} - LHV_{dev} - \frac{LHV_{char} x_{char}}{1-x_{ash}}}{x_{vols}(1-x_{ash})} \qquad \text{Eq(22)}$$

LHVs for typical pyrolysis gas species are presented in Table 6. As previously explained, hydrocarbons are simplified to CH_4 and C_6H_6 and the LHV of other hydrocarbons range between these species.

Table 5: LHV values for pyrolysis gases.

Specie	LHV(MJ/kg)
CO	10.1
H_2	119.96
CO_2	0
H_2O	0
CH_4	50.01
C_6H_6	37.0
LHV gas mixture	**16.13**

The molar fractions of pyrolysis gases can then be obtained from Equation 23, with the given LHV values. However, there are 6 unknowns and 4 equations, hence 2 more assumptions have to be made. According to [41], there are 0.08 kg H_2O released by volatiles per kg daf fuel, which is an assumption made in this project. The other assumption is that around 0.03 kg tars per kg daf fuel is produced. Then only CO, CO_2, H_2 and CH_4 are unknown and the system can be solved.

$$LHV_{pyro} = \sum_{i=1}^{n} n_{i,pyro} M_i LHV_i \quad \text{Eq(23a)}$$

$$n_C = n_{CO} + n_{CO_2} + n_{CH_4} + 6C_6H_6 \quad \text{Eq(23b)}$$

$$n_O = n_{CO} + 2n_{CO_2} + n_{H_2O} \quad \text{Eq(23c)}$$

$$n_H = 2n_{H_2} + 2n_{H_2O} + 4n_{CH_4} + 6n_{C_6H_6} \quad \text{Eq(23d)}$$

The corresponding concentration of pyrolysis gas is presented in Table 6 The CO and H_2 content are the highest on a molar basis, in order to yield the correct LHV_{pyro}. Comparing the results here with the ones from Table 3, the CO and H_2 content have the highest molar fractions but in this case, the CH_4 content is higher than CO_2, which is different from Table 3. That is mainly due to that LHV_{pyro} is higher in bark than in biomass in general, which leads to that a larger share of carbon species must be present as a combustible rather than CO_2.

Table 6: Pyrolysis gas concentrations

Specie	Mass-%	Mole-%
CO	48.3	34.1
CO_2	21.7	9.8
H_2	2.8	27.8
H_2O	10.4	11.5
CH_4	12.8	15.8
C_6H_6	3.9	0.98

This composition of pyrolysis gases was then used in all modelling cases. It is furthermore assumed that all pyrolytic compounds are released which is reasonable since the temperature is well above 450-550 °C.

2.4 BED MATERIAL FLOW AND SIZE OF GASIFIER

With all information about inlet streams and reactions were set up, the mass and energy balances could be solved. To resolve the energy balance the gasifier requires

heat input from the combustor, which was solved by setting the bed material heat flow to be as large as the heat demand in the gasifier. The energy balance of the bed material flow is seen in Equation 24. Values for heat capacity and density of the bed material are approximated with the values for silicon.

$$\dot{Q}_{bm\ from\ combustor} = \dot{n}_{SiO_2}\left(C_{P,A,SiO_2}\left(T_{combustor} - T_{gasifier}\right) + \frac{C_{P,B,SiO_2}\left(T^2_{combustor} - T^2_{gasifier}\right)}{2}\right)$$

$$\rightarrow \dot{m}_{between\ bed} = \frac{\dot{Q}_{bed\ material\ from\ combustor} * M_{SiO_2}}{C_{P,A,SiO_2}(T_{combustor} - T_{gasifier}) + \frac{C_{P,B,SiO_2}(T^2_{combustor} - T^2_{gasifier})}{2}} \qquad \text{Eq(24)}$$

2.5 RESIDENCE TIME IN GASIFIER

Residence time and temperature in the gasifier is a crucial parameter to how much of char will gasify. According to results obtained at Chalmers under comparable conditions it is assumed that 10 % of all char is converted in the gasifier. The rest will follow the bed material circulation to the combustor where it gets combusted.

The residence time for the fuel in the gasifier can be calculated according to Equation 25. The total mass of the bed in the gasifier is achieved from the bed volume and bulk density of the particles whereas the mass flow between beds are provided from the mass and heat balances in Section 2.1 and 2.4.

$$\tau_{fuel} = \frac{m_{g,bed}}{\dot{m}_{between\ beds}} = \frac{A_{bed} L_{bed} \rho_{bed,bulk}}{\dot{m}_{betweenbeds}} \qquad \text{Eq(25)}$$

The area is set to be 2*1 m. The resulting residence times, shown in Table 10 are dependent on moisture content since it demands lower flow of bed material between the beds for higher moisture contents. This calculation assumes that there is perfect mixing of bed material in the gasifier. It is however most likely that there are stagnant zones in corners. It is also necessary to add fuel as far from the bed material outlet as possible, forcing the fuel to travel as far distance as possible to leave the gasifier. A higher moisture content will therefore decrease the fraction of gasified char.

Table 7: Residence times in the gasifier for different moisture contents

Moisture content (%)	Residence time(s)
0	772
10	661
20	561
30	468
40	384
50	306

3 Cold flow model experiments of a DBFB reactor

3.1 SCALING DOWN A CONVENTIONAL BFB REACTOR TO LAB SCALE SIZE

Glicksman has provided a way of scaling a fluidized bed reactor from an operating full-scale model to a cold experimental model in a promising way [42]. A set of dimensionless number are suggested to remain constant between the hot (full scale) and the cold scaled system in order to give the same fluidization pattern. Maintaining these parameters constant has shown to give very similar flow patterns in experiments and in CFD simulations [43] [44].

Table 8 shows the scaling parameters to be kept constant. The procedure of scaling is first to achieve all necessary data from the full-scale reference. Then a gas for the experimental model should be chosen, providing density and viscosity of the fluid. That will give the required density of the particles by the density ratio. By combining the Froude and Reynolds number the scaling factor can be achieved, shown in Equation 26. FS means full scale and EM experimental model whereas m is the scaling factor. Finally, the remaining parameters can be achieved as described in Equation 27.

Table 8: The full set of Glickman's dimensionless scaling parameters. u_0 is the superficial velocity, g is the gravity constant, D is the diameter or width of the bed, ρ_p is the particle density, ρ_f is the fluid density, d_p is the particle diameter, μ_f is the fluid viscosity, G_s is the mass flux of bed material, L is the height of the bed, φ is the sphericity constant and PSD is the particle size distribution.

scaling parameter	Equation	Name
1	$\frac{u_0^2}{gD}$	Fr
2	$\frac{\rho_p}{\rho_f}$	Density ratio
3	$\frac{\rho_f u_0 d_p}{\mu_f}$	Re_d
4	$\frac{\rho_f u_0 D}{\mu_f}$	Re_D
5	$\frac{G_s}{\rho_p u_0}$	Mass flux ratio
6	$\frac{L}{D}$	Bed dimensions
7	Φ	Sphericity
8	PSD	Particle size distribution

$$m = \frac{L_{FS}}{L_{EM}} = \left(\frac{\rho_{g,FS}\mu_{EM}}{\rho_{g,EM}\mu_{FS}}\right)^{2/3} \quad \text{Eq(26)}$$

$$\frac{u_{0,FS}}{u_{0,EM}} = \frac{t_{FS}}{t_{EM}} = \left(\frac{L_{FS}}{L_{EM}}\right)^{1/2} = m^{1/2} \quad \text{Eq(27)}$$

However, Glicksman did also present a simpler version of scaling parameters where parameter 3 and 4 are excluded and instead the parameter $\frac{u_0}{u_{mf}}$ is introduced. u_{mf} is the minimum fluidization velocity which will be further explained.

The minimum fluidization velocity can be theoretically achieved by deriving the Ergun Equation, Equation 28 [43], and creating a force balance on the bed, shown in Equation 29 assuming steady state [44]. The Koceny-Carman equation can then be formed to express the minimum fluidization velocity, shown in Equation 30, valid for Reynolds numbers lower than 20 [43].

$$\frac{\Delta P}{\Delta x} = 150\frac{u_0\mu_f(1-\epsilon)^2}{D_p^2\epsilon^3} + 1.75\frac{\rho u_0^2(1-\epsilon)}{D_p\epsilon^3} \quad \text{Eq(28)}$$

$$Upward\ force\ on\ the\ bed = \Delta pA \quad \text{Eq(29a)}$$

$$Weight\ of\ particles = (1-\epsilon)(\rho_p - \rho_f)gAL \quad \text{Eq(29b)}$$

$$=> \Delta P = (1-\epsilon)(\rho_p - \rho_f)gL \quad \text{Eq(29c)}$$

$$u_{mf} = \frac{D_p^2(\rho_p-\rho_f)g}{150\mu}\frac{\epsilon^3}{(1-\epsilon)} \quad \text{Eq(30)}$$

The porosity, or void fraction, ϵ can be obtained from Equation 31 via the density of the bed when fluidized, ρ_{bulk}, which can be obtained from the mass of the bed material and the volume of the fluidized bed.

$$\epsilon = 1 - \frac{\rho_{bulk}}{\rho_p} \quad \text{Eq(31)}$$

The minimum fluidization velocity, u_{mf} can also be obtained from experimental trials. The bed height will increase when increasing the superficial velocity at levels below the minimum fluidization velocity. When the superficial velocity equals u_{mf} the bed height starts to increase and does so with a linear pattern with increasing superficial velocity [46].

The necessary parameters for the scaling procedure are shown in Table 9. The calculated density for the experimental model is 10223 kg/m^3, which is t of importance in scaling parameter 2, the density ration between bed and gas., As a material with that density was not available, instead bronze was used with a density of 8900 kg/m^3 which is close enough to create reliable results.

Table 9: Parameters from scaling. The bold numbers are calculated from scaling, the others found in literature or given from existing setups.

Parameter	Full scale(Skärblacka)	Experimental model(Chalmers)
u_0	0.366 (m/s)	0.071 (m/s)
ρ_f	0.3121 (kg/m^3)	1.204 (kg/m^3)
ρ_p	2650 (kg/m^3)	8900 (kg/m^3)
μ_f	45.72 (µPas)	18.2 (µPas)
u_{mf}	0.309 (m/s)	0.058 (m/s)
d_p	950 (µm)	111.4 (µm)
L	100-150 (cm)	3.75-5.625 (cm)
A	8*8 (m*m)	0.3*0.3 (m*m)

The transferred bed material measured in the experiments needs also to be translated back to the full plants size. That will not be made through scaling equations but to the mass balance equations. Since the air flows scaled down according to scaling laws, the corresponding mass flow of air in the experimental model is known. From the energy and mass balances, a mass quote between bed material circulation and fluidizing agent can be obtained. This quote will be valid even for full scale.

The correlation equation is shown in Equation 32. The mass flow of fluidizing agent in the full-scale model is 5.9 kg/s and the air flow in the experimental model 0.0077 kg/s, which implies a factor of 771, meaning that if the experimental model transfers bed material of 1 g/s, it corresponds to 0.771 kg/s in the full-scale model.

$$\frac{m_{between\ beds,FS}}{m_{fluidizing\ agent,FS}} = \frac{m_{between\ beds,EM}}{m_{air,EM}} \qquad \text{Eq(32)}$$

A quota between the full-scale model volumetric flow and the experimental model volumetric flow is shown in Equation 33. This quota can be used to express the extra fluidization flow from the experimental model into the required volumetric flow in the full-scale model.

$$q_{vol} = \frac{\dot{V}_{fluidisation,FS}}{\dot{V}_{fluidisation,EM}} = \frac{23.42}{0.0064} = 3672 \qquad \text{Eq(33)}$$

3.2 EXPERIMENTAL INVESTIGATION OF MINIMUM FLUIDIZATION VELOCITY

The bed material sand that is used at BillerudKorsnäs is Baskarp B95 has an average diameter of 950 µm. That is a rather large particle diameter compared to other fluidized beds and that resulted in a high minimum fluidization velocity. To investigate if the scaling laws were valid in this range of particle diameter, it was decided to test the minimum fluidization velocity of the bed material. B95 was imported from the company Sibelco Nordic AB.

The experimental setup is shown in Figure 6. The figure shows how air is led through a heated pipe and in to the tubular reactor. Inside the reactor the air flows through a porous plate and then through the bed material to exit the top. The amount of bed material was chosen so that the upper layer would be in between measurement point P1 and P2. However, as the bed is fluidized it will increase its height and most likely interfere with P2. What is not shown in the figure is that the tube is placed inside an electric oven heating its inside to a temperature around 710 °C. Since T3 and especially T1 is placed at points of interest the temperature inside the tube can be assessed.

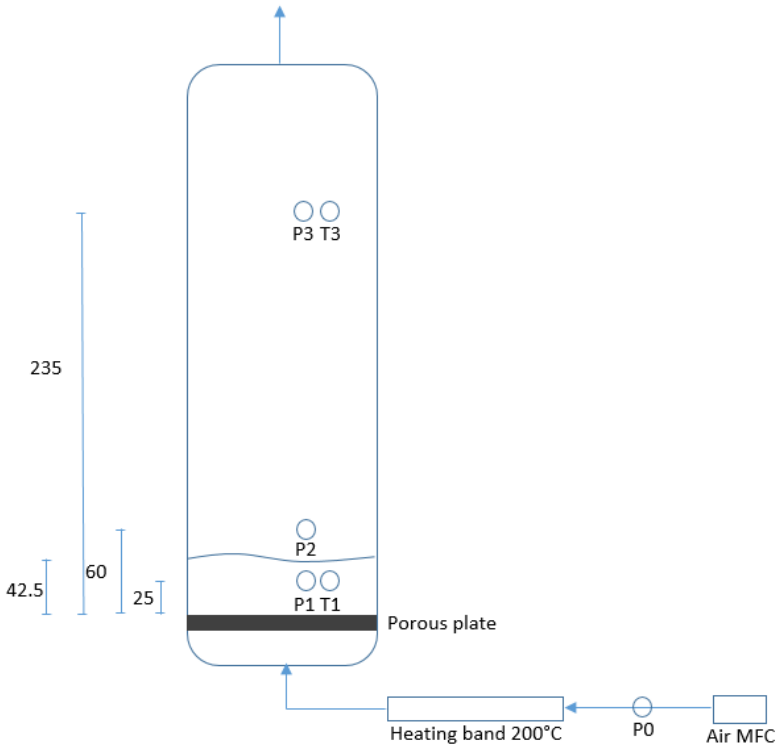

Figure 6: A simplified scheme of the setup of the u_{mf} test. The heights are shown in mm.

Since the mass flow controller readings gives the volumetric air flow in cold conditions, it has to be recalculated to the conditions inside the tube. The calculations were performed as in Equation 34, derived from the ideal gas law.

$$V_C T_C(K) = V_H T_H(K) \qquad \text{Eq(34)}$$

The pressure measurements P0 and P1 could give the pressure drop over the distributor plus the pressure drop over the first 25 mm of the bed. For determining u_{mf} experimentally, it is usually required to measure the pressure drop over the porous plate. Due to the fact that P1 is not located just above the plate, it was decided to not perform those calculations in this report. What was more interesting was instead to measure the pressure difference between P1 and P3 as well as P1 and P2.

The procedure was to heat up the tube and then run tests with different cold volumetric flows. 6 measurements every second for 30 seconds of stable operation were taken at each volumetric flow, which would provide a stable value for the pressure drop measurements.

The resulting pressure drops of P1-P2 and P1-P3 is shown in Figure 7. u_{mf} is obtained when there is no increase in pressure drop with increasing u_0. However, the amount of bed material between the measurement points is not equal during the experiments since P1 is located in the middle of the bed. As the bed gets more fluidized the material moves upwards and therefore increase the content of bed material between the measurement points. More material gives larger pressure drop. Observing Figure 8 this pattern can be spotted. The pressure drop increases rapidly at low u_0s and at around 0.3-0.4 the increase of pressure drop reduces. Even though the pressure drop is changing less, there is still an increase which can be explained by this bed material gain

between the measurement points. From this figure it is therefore suggested that u_{mf} is located between 0.3 and 0.4.

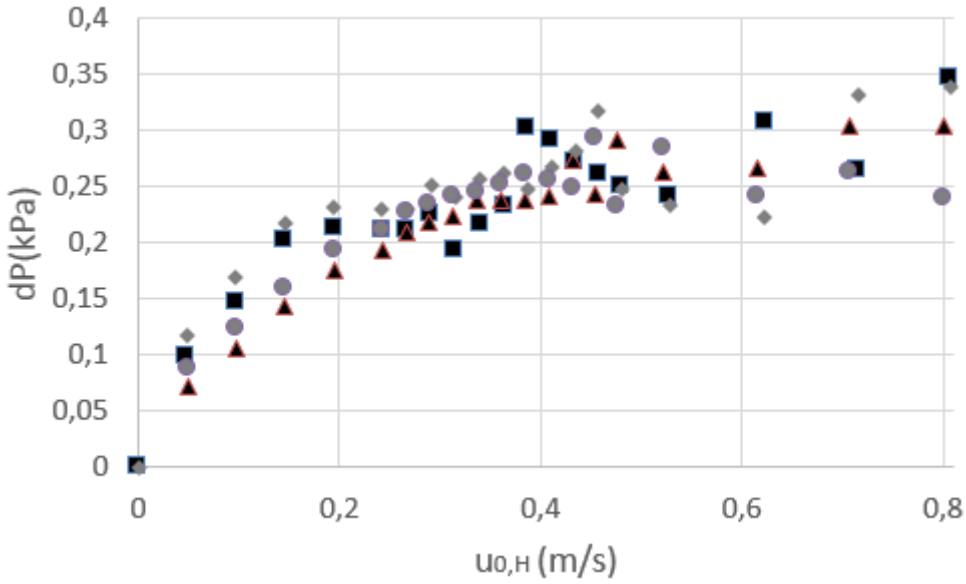

Figure 7: Pressure drop (kPa) vs $u_{0,H}$ (m/s). The black plots represent P1-P2 and the grey P1-P3.

Another indication for the quality of the fluidization is the pressure drop presented in Figure 9 for measurement of P1-P3 over time. As excess gas, beyond u_{mf} passes through the bed as bubbles and as those bubbles create large pressure differences within small time frames the region above u_{mf} can be identified as well by the measurement of those fluctuations. When increasing the flow, it is apparent that the bed begins to bubble at around 14-16 l/min and at the decreasing side it appears to be around 16-18 l/min. These flows correspond to an u_0 of 0.33-0.43 m/s, which is in accordance with the suggestion made from the analysis of the slope of dp over the bed.

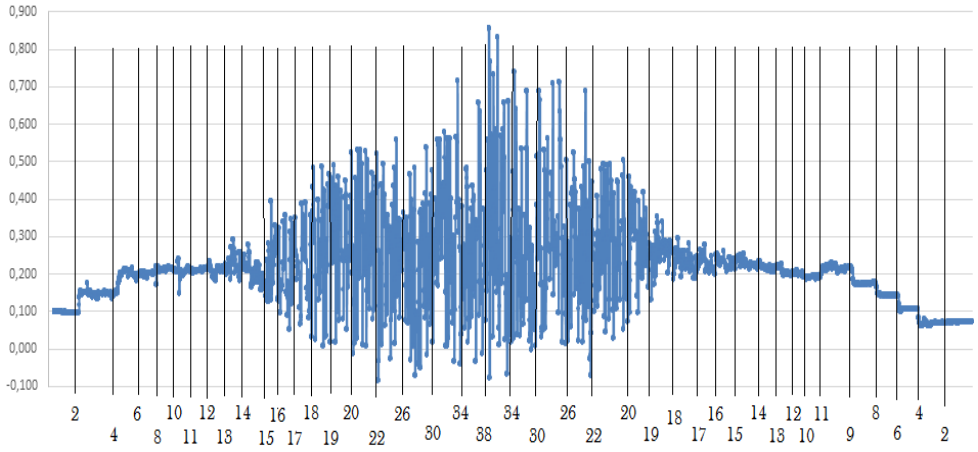

Figure 8: Pressure drop of P1-P3 (kPa) vs time (min). The x-axis is marked when flow was changed (l/min)

Comparing the onset of fluidization for both methods with what was tested for the bronze material used in the cold flow experiments, which was 0.305 and 0.310 m/s, the

deviation is under 10% and the agreement is considered to be sufficient to generate reliable results.

3.3 SETUP OF COLD FLOW EXPERIMENTS

The tests were performed in a 30*30cm reactor representing the scaled squared cross section of the installation at the Skärblacka site. Gas was introduced through holes in the bottom plate with a diameter of 3 mm in diameter and it was 16*16 of them in the bottom area. Above that plate, a net was placed preventing the sand could from falling through the holes. Due to uneven fluidization distribution, another plate was put above the net, providing a higher pressure drop but improved the fluidization distribution. The hose with extra fluidization air had 6 holes with diameter of 3 mm with a 1 cm gap between them. That hose was put on the highest plate about 2 cm from the bed material outlet. The air flows were controlled manually by flow meters where the main one reached between 0 and 600 l/min and the extra air used a flow meter that reached between 0 and 50 l/min. The cold flow model at the bed material outlet position without bed material inserted is shown in Figure 10. The width of the opening was 5 cm, 133 cm correspondingly to the full-scale combustor.

In Table 13 the setup of experiments is shown. In each experiment, superficial velocities of 315 (u_{mf}), 383 (u_0 at BillerudKorsnäs correspondingly), 450, 500, 550 and 600 l/min were tested. The experiments were carried out several times in order to investigate repeatability. The bed height (L) in BillerudKorsnäs varies from 1.0-1.5 m and that corresponding bed height in the experiments is 3.75-5.625 cm, therefore the extreme cases were investigated. The bed material leaving the chamber went through a funnel and into a bucket placed on a scale. The scale was a PS 10100.R2 precision balance of the brand Radwag, with a readability of 0.01 g. The scale was connected to a computer with a software receiving the data from the scale.

The outlet position had a height of 2 cm above the bed under non-fluidizing conditions, correspondingly 53 cm for the full-size scale. The importance of the outlet position in relation to the bed height was investigated in one experiment where the height was increased by 1 cm, or 26.67 cm correspondingly. Since the outlet of the retrofitted gasifier needs to be placed at a lower position than the combustor outlet, it would be preferred to have an enough height difference to guarantee steady flow patterns through the gasifier. To generate results valid for any size of opening the relationship between the bed material flows to the opening width was tested as well experimentally.

Figure 9: Setup of the hose for extra fluidization shown in the cold flow model combustor chamber when no bed material is added.

In each experiment 90 seconds of measuring were taken with a measuring interval of 1 measure per second. The chamber was filled with 100 g portions of bed material for every 100 g leaving the chamber during the experiments. After each experiment was finished, the remaining sand was filled in order to have the same amount at the start of each experiment. The bed material chosen was bronze due to its high particle density, as described in Section 3.1, and the mean particle diameter was obtained at 101 μm. The correct mean particle diameter should be 111 μm so the bed material was sieved so that the smallest particles were removed which increased the mean particle diameter to the correct value, the measurements shown in Appendix A1.

Table 10: Setup parameters for the experiments

u_{extra} (l/min)	Bed height L(cm)	Number of measurements	Comment
0	3.75	1	-
10	3.75	1	-
20	3.75	2	-
30	3.75	4	-
40	3.75	3	-
50	3.75	2	-
20	5.625	1	-
30	5.625	2	-
40	5.625	2	-
30	3.75	1	Half outlet width
40	3.75	1	1 cm higher outlet position

The cold flow model combustor chamber is shown in Figure 11. The sand is filled with a height of 3.75 cm and the distance between the top of the bed and the outlet is 2 cm.

Figure 10: The cold flow model combustor chamber with sand and no fluidization.

3.4 EXPERIMENTAL INVESTIGATION OF BED MATERIAL TRANSFER BETWEEN TWO BFBS

The bed material transfer between two bubbling fluidized bed was investigated in this project by means of a downscaled model of a BFB to assess the feasibility to provide heat to a gasification reactor by in such an arrangement. The main operating parameters are presented in Section 3.1 and the parameters that were changed explained in Section 3.3.

The experiments showed that there was no specific change in bed material flow over time, so the flow was considered to be constant. Therefore, the mean values between start and stop of one run were utilized to calculate the flow.

All results from the experiments with 3.75 cm bed height are shown in Figure 11. For 0 and 10 l/min extra fluidization results in negligible bed material transfer whereas the transfer for 20 l/min is small, but significant and similar in both experiments. The transfer for 30 l /min is rather spread out between the experiments and the spreading increased with higher flows, particularly for 40 l/min and for 50 l/min. this is in accordance with the observation of less stable flow conditions for operation of the flow meters close to their maximum (50 l/min

Generally, an increase with increasing fluidization of the main bed can be observed. Some experimental series such like 30a and 50c display large variations within

themselves and are therefore excluded from further evaluation. For higher extra fluidization the spreading within the runs and between the runs of similar settings increase and both 40 and 50 l/min extra fluidization create results in the same range.

In almost all experiments, increasing normal fluidization flow increases the bed material transfer with only a few exceptions. However, to achieve a more efficient bed material transfer it is better to increase only the extra fluidization flow. Going from 10 to 40 l/min extra fluidization increases the bed material flow with several orders of magnitude instead of only double the flow when going from 383 to 600 l/min normal fluidization flow. Such an increase in fluidization flow would imply a larger fuel flow and therefore heat demand. It is therefore suggested to only consider normal fluidization flows of 383 l/min, which is the one used in Skärblacka, and investigate the extra fluidization in that part.

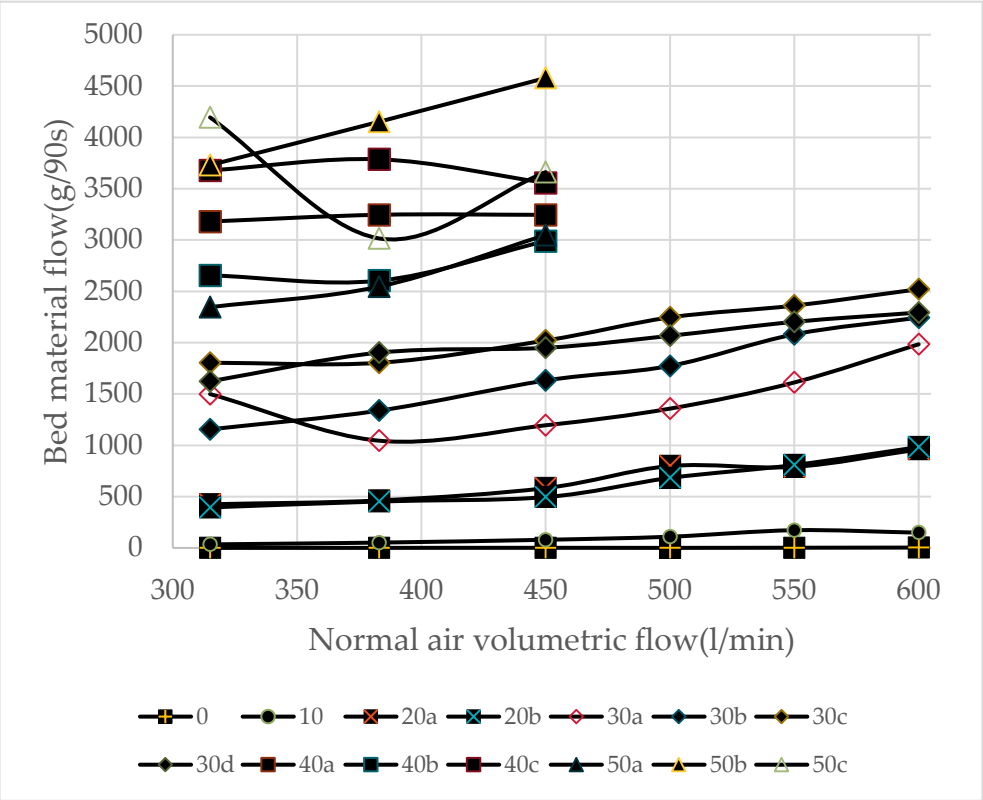

Figure 11: Bed material transfer after 90 seconds of running for the experiments with bed height of 3.75 cm. 10, 20, 30, 40 and 50 correspond to the volume flow of the extra fluidization in l/min while a-c is indication replicas at one condition

The results from the experiments are shown in Figure 12. The amount of bed material flowing out from the experimental model after 90 seconds of operation is plotted against increasing extra fluidization, where the normal volumetric flow was 383 l/min, the corresponding volumetric flow that is used in Skärblacka. The higher the extra fluidization the higher the bed material flow, except from 40 to 50 l/min where an extra fluidization increase seems unnecessary. The results vary significantly for the same amount of extra fluidization, which might be that the bed has not a homogeneous fluidization through the whole bed, where it in some experiments may be higher fluidization at the outlet and lower in other. Another reason might be that the volumetric flow of extra fluidization was not exactly the same since the flow meter

might show unreliable values. This experimental data provides therefore a span of bed material flow.

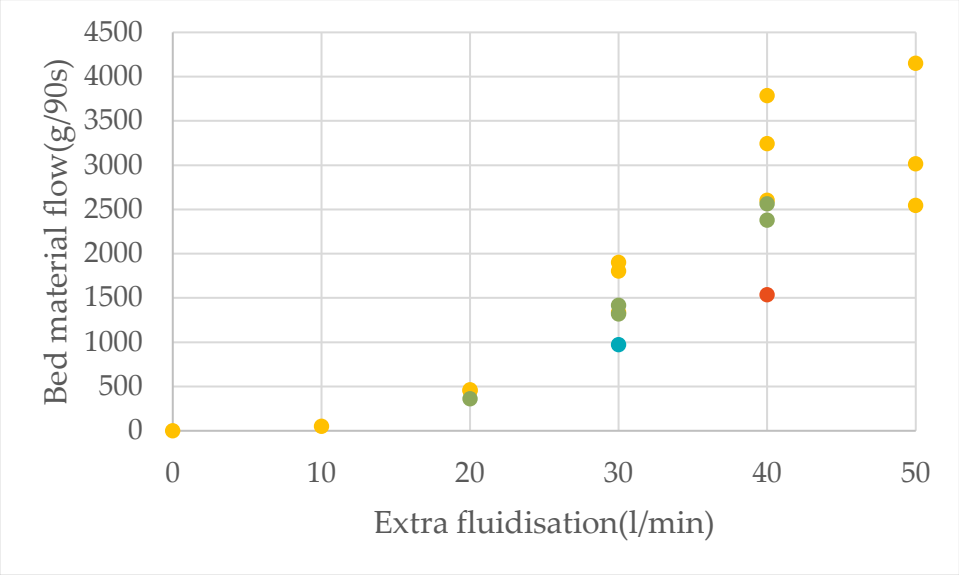

Figure 12: Bed material flow from the experimental chamber from experiment with different extra fluidization. Bed height = 3.75 cm, ●yellow (reference) 1m bed height, ●blue 50% reduced opening, ● red 50 % increased exit wall height, ●green 1.5 m bed height.

The resulting bed material transfer for the cases with a higher bed, 5.625 cm, is shown in Figure 13. The results are more even than with the lower bed. The transferred amount of bed material is similar to the experiments with lower bed, however it can be observed that the transferred bed material is somewhat lower with the higher bed height.

The width of the outlet was also put to half to investigate the correlation between width and bed material transfer. A case with 30 l/min was performed and the transferred bed material after 90 seconds was 973.95 g. The comparison between the other bed material transfers for the same extra fluidization is shown in Table 14. It is seen that the bed material transfer is not 50 %, but on average 64 %. However, considering the variation within the results and the fact that only one experiment on half the width was performed, indications are that the bed material transfer is linearly dependent on outlet width.

Table 11: Bed material transfers with extra fluidization of 30 l/min compared with a case with half the outlet width.

Run	Bed material transfer(g/90s)	Corresponding fraction of half the width
+30, ½ width	973.95	100 %
+30 b	1337.61	72.8 %
+30 c	1803.89	54 %
+30 d	1902.64	51.2 %
+30 average	1522.18	60 %

The height distance between the outlet and the top of the bed has always been 2 cm. A test where that distance was increased to 3 cm was made for a case with 40 l/min extra fluidization. The transferred bed material over 90 seconds was 1537 g and its comparison to the other tests can be found in Table 15. It is seen that a higher distance between outlet and bed has a large impact on bed material transfer. By increasing that distance from 2 to 3 cm, the transfer is reduced by more than 50 %. Only one experiment was made with the higher outlet-bed distance and the result might indicate a trend, showing that the bed material transfer is greatly reduced by higher distance can be adopted.

Table 12: Bed material transfer for experiments with 40 l/min extra fluidization compared with a case with higher outlet-bed distance

Run	Bed material transfer(g/90s)	Corresponding fraction of the higher outlet-bed distance
+40, 3cm outlet-bed distance	1537	48 %
+40 a	3245	101 %
+40 b	2603	81 %
+40 c	3786	118 %
+40 average	3211	100 %

4 Results

4.1 ENERGY BALANCE CALCULATIONS

In this project, two different parameters have been varied to investigate the energy demand of the gasification, the moisture content of the bark and the size of the gasifier. The energy demand translates directly to the required bed material flow to maintain the temperature levels in the system. The moisture content has been varied between 0 and 50 % in the gasifier to see the effects on how drying affects the heat demand. The size of the gasifier has been varied between 4 and 18 MW, in terms of energy content in the product gas. Those two parameters coupled to the achievable material flow, derived from cold flow experiments, confine the possible design range.

The size of the combustor was practically set from the given data since the flow of fluidizing agent was given and was held at a steam production of 30t/h corresponding to around 20-22 MW. As the limitations of in terms of heat transfer in the boiler was not accessible under the time frame of that project those values are kept constant. However, one has to keep in mind that for the periods with low heat demand from the paper mill a lowered heat output would be beneficial.

The required bed material flow between the gasifier and combustor for different moisture contents is plotted against increasing gasifier size in Figure 6. The lowest line represents cases with 0 % moisture content and the highest line represents cases with 50 % moisture content. Logically, the largest moisture content and largest gasifier size requires the highest bed material flow.

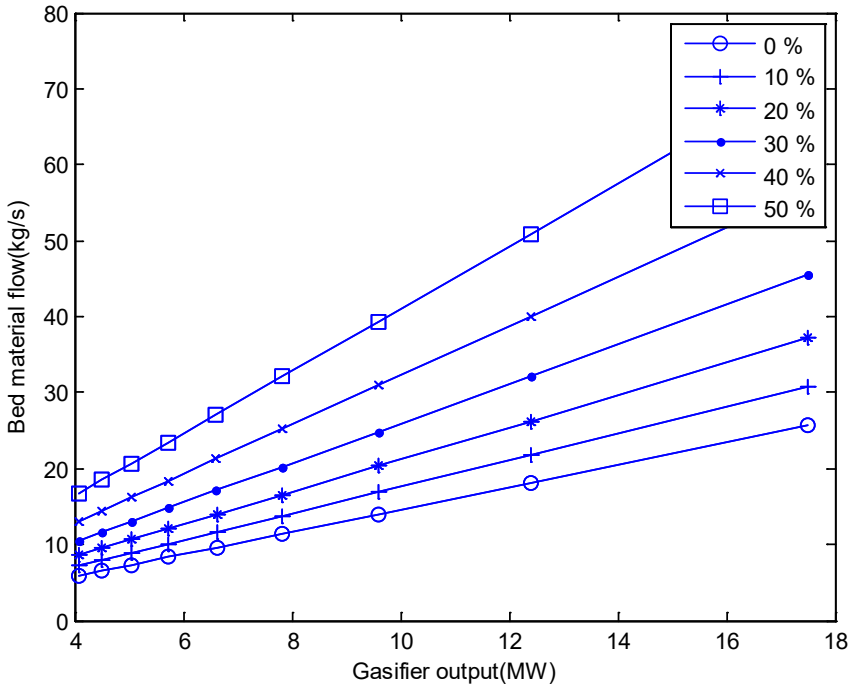

Figure 13: Required bed material flow (kg/s) for different moisture contents vs gasifier size (MW)

At constant material flow the possible gasifier size decreases with 15-20% for each 10% increase in fuel moisture in the size range shown here, e.g at 20kg/s bed material flow a gasifier of 10 MW_{gas} can be driven with a fuel with a moisture content of 20 %, while the same number is 5 for a fuel moisture of 50 %.

4.2 PRODUCT GAS LHV

Depending on the downstream treatment of the gas the heating value will vary as in case of cooling the containing steam and condensable hydrocarbons will be removed. This will be the case if higher energy density is required or longer distances between gas production and consumption need to be bridged. If the main utilization is direct combustion in for example a lime kiln a gas temperature above 250 °C is preferred and condensation of steam and condensable hydrocarbons is avoided.

The resulting product gas composition is shown in Table 13. The table shows results for both 20 and 50 % moisture content and, logically, the H_2O concentration is higher and all other species lower when the moisture content is high. In these examples, a steam to fuel ratio, SFR, of 0.5 is used, which is a value that gives reasonable superficial velocities. The LHV of the 20 % moisture content case is 8.4 MJ/kg and 5.6 MJ/kg for the case with 50 % moisture content. According to [31] the LHV at Joutseno is kept at 5-7 MJ/kg and can keep running of the lime kiln possible. Thereby is the 50 % moisture content case is relatively low. Comparing with results from large scale bark gasification it is apparent that the model overestimates the lower heating value per kg gas. The reason for this are the catalytic effects provoked by the ash species present in the fuel enhancing both the WGS reaction and fuel conversion. This results in a dilution of the gas with CO_2 originating from above mentioned reactions. The gas yield, in terms of $MJ_{gas}/MJ_{fuelinput,}$ however, are higher in those cases.

Table 13: dry product gas composition in mole-% leaving the gasifier, which holds 800 °C, *including light hydrocarbons calculated as methane

Specie		Composition 20 % moisture	Composition 50 % moisture	GoBiGas [18] Olivine	Chalmers Silica sand
CO	Vol%	36,1	34,3	17-21	26,6
CO_2	Vol%	12,2	13,5	23-25	25,6
H_2	Vol%	35,1	35,9	39-43	30
CH_4	Vol%	15,6	15,4	7,1-8,7 (11,2*)	12,1 (16,5*)
tar	g/Nm^3			8-15	>50
LHV_{humid}	(MJ/kg)	8.36	5,6		
LHV_{dry}	(MJ/kg)	17,9	17,9	12,8	12,7

4.3 MATERIAL CIRCULATION AND HEAT BALANCE

To assess the possible heat transfer through bed material circulation between the combustor and gasifier in the full-scale chamber at Skärblacka downscaled cold flow experiments were performed. The bed material flow from those experiments can be converted into the corresponding bed material flow expected at Skärblacka.

Converting the results of the experiments into the sizes of the modelled DBFB system was shown in Section 3.1 where a factor converting bed material flow in Equation 32

and volumetric flow quote in Equation 33 were shown. The results from Section 3.4 with axes that corresponds to the modelling sizes is shown in Figure 15. The bed material flow is shown per meter of outlet opening in the full-scale combustor. The figure shows that a high extra fluidization can give significant high bed material flow. With local extra fluidization of 10% the corresponding bed material flow is 16-24 kg/s per meter of outlet opening.

For a furnace size of 8x8m as at the Skärblacka site openings wider than one meter are feasible. The specific design, and as a consequence the width of the opening, will depend on the available space. While the inlet to the gasifier should be as large as possible, for a large system, the return opening can be kept reasonably small, as the material does not flow over a weir but through a loop seal.

The distance between the top of the non-fluidized bed and the outlet has been kept at 2 cm, which corresponds to 0.5 m at Skärblacka. That height difference is essential so the bed material from the gasifier to the combustor flows naturally through another outlet opening.

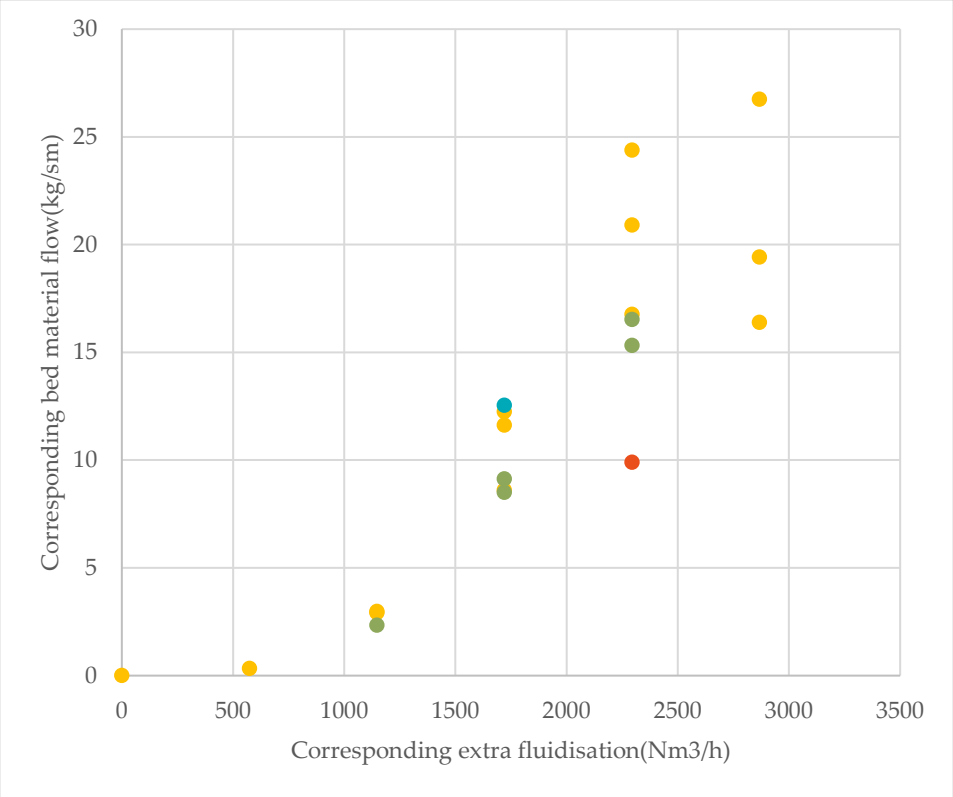

Figure 14: Bed material flow per meter of outflow opening from the experiments with different extra fluidization in its corresponding units for the paper plant, ●yellow (reference) 1m bed height, ●blue 50% reduced opening, ● red 50 % increased exit wall height, ●green 1.5 m bed height.

The required width can then be assessed combining the heat balance calculations for a given gasifier size and moisture content with the achievable material flows (Figure 14). In Figure 15 the required material circulation is plotted against the gasifier output for different fuel moisture. The red area represents the possible operational points for a

two-meter-wide opening. Under those conditions a gas production of almost 18 MW is possible for 20% moist fuel or almost 10 MW for 50% moist fuel.

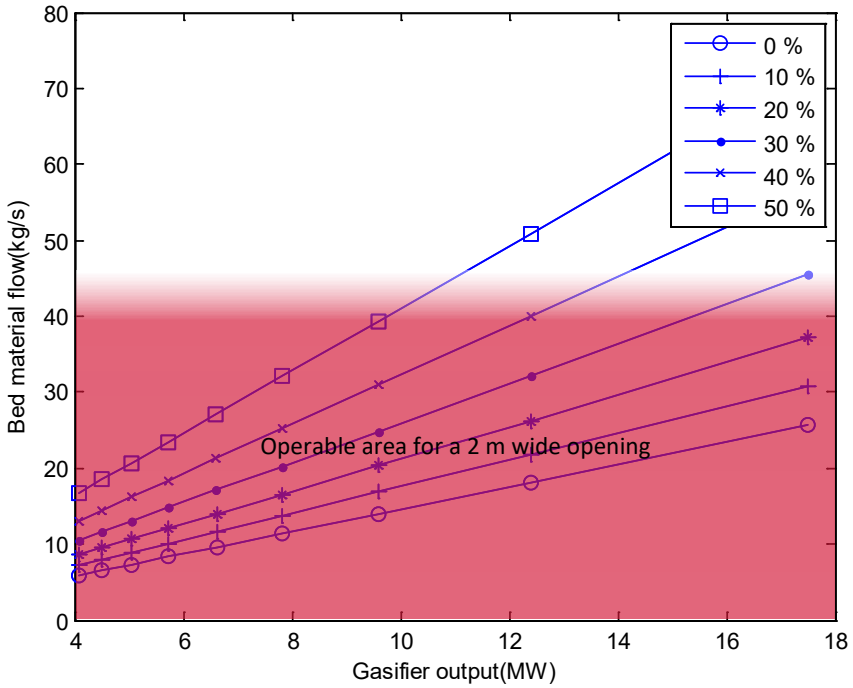

Figure 15: Required bed material flow against gasifier output for different moisture contents

The resulting heating demands are shown in Table 8, for three different cases, 17.5MW$_{gas}$ gasification with 50% and 20% fuel moisture respectively and a gasification halve the size with 50% fuel moisture. From top to down the table gives inside on the fuel input as lower heating value on moist basis, the heat demand of the gasifier, the heat exchanged between the beds in form of hot sand and char and the energy output from both the gasification and the combustor. Mentionable is the moisture content of the gasifier fuel which poses the biggest heat demand by far. The heat demand, which needs to be covered by heat transfer between the combustor and the gasifier in form of circulating sand. On an energy basis this heat is compensated for through the returned char, however, there might be a fluid dynamic limitation, favoring a pre- dried fuel.

Considering the output of the gasifier one has to keep in mind that not all sensible heat will be recovered, depending on the downstream usage. For direct combustion in the lime kiln only the sensible heat down to 250 °C will be recovered directly, the rest will be found in the flue gases of the kiln. For utilization in a more demanding burner system e.g. drying of paper, a full condensation of steam and formed hydrocarbons of the gas is required and the heat below 250 °C will be recovered at the steam condensation temperature and below.

Table 14: Heat requirements in the modelled DBFB system for different cases

		Gasifier Size, fuel moisture		
		17,5 MW 50%	**9,7 MW 50%**	**17,5 MW 20%**
Fuel Input [MW]	Combustor (LHV moist 50%)	-17,5	-21,4	-17,3
	Gasifier (LHV moist 20 or 50%)	-24,4	-13,2	-26,5
Heat demand gasifier [MW]	Sensible heat dry gas (25-750 °C)	1,38	0,77	1,39
	Evaporation of moisture and sensible heat (25-750 °C)	5,37	2,98	1,36
	Sensible heat fluidization steam (150-750 °C)	0,95	0,48	0,88
	Heat of reaction gasification and WGS @750 °C	0,28	0,14	0,28
Heat transfer [MW]	Net-heat transfer with bed material from combustor-gasifier ΔT=100 °C	8	4,6	4,3
	Char from gasifier to combustor	9	5	9,1
Gasifier output [MW]	Product gas LHV	17,5	9,7	17,6
	Sensible heat product gas Temperature level 200 -25°C	7,72	4,2	3,63
Boiler output [MW]	Steam produced	18,5	21,8	22,1
	Heat below 100 °C	2,4	3	2,4

5 Conclusion of the project

This project has investigated the possibilities to add a gasifier onto an existing bark BFB combustor in paper plants by means of weir. The bark boiler of BillerudKorsnäs Skärblacka has been used as a reference plant, importing data and operating conditions from there. Investigation has been made on previous bark gasification plants, DFBG plants and bark composition papers giving reasonable predictions of resulting outputs of this retrofitted plant. Mass and energy balances have been established over this system in order to evaluate how much gas that can be produced, what quality the gas will have and how much energy is required in both combustor and gasifier to keep the energy balance in each chamber. The bed material transfer has been exclusively investigated in cold downscaled model experiments as well as an experimental of minimum fluidization velocity of the bed material at Skärblacka which have been compared with calculations made. The obtained bed material flow was compared with the heat and mass balance models in order to examine possibilities of implementation.

It has been discovered that the proposed setup of extra fluidization to the combustor can definitely provide a bed material flow high enough to reach the energy balance in the gasifier. The extra fluidization stream, which should constitute of recirculated gas, will require extra energy heating the gas, but will have only a small contribution on energy demands.

While the heat demand for the endothermic reactions of pyrolysis and gasification is relatively small in comparison the evaporation of moisture and the heating of the fluidization steam is to consider.

For the investigated cases a gasifier output almost as high as the combustor output is reachable for pre- dried fuel (20%) in the gasification. Such dried fuel will also give a higher LHV of the product gas, which is favorable for all direct uses of product gas, e.g. in the lime kiln.

For higher moisture content the possible size of the gasifier decreases naturally as heat demand for evaporation of the moisture is dominating and will affect the heat balance in the furnace. Another effect on the operation of the boiler is the added amount of char from the gasifier which will likely affect the temperature distribution in the furnace as less volatiles are released. Simultaneous less secondary air is required as more fuel (char) is burning inside the bed which might allow to reduce the load of the boiler beyond the current level. Those two effects should be investigated further as they could reduce unnecessary heat production during the warm periods of the year. However, one should keep in mind that requirements for the heat exchanging surfaces, especially in the furnace wall, need to be met.

An alternative scenario would be to run the gasifier in pyrolysis mode (at 500 °C) and to extract the char. In this scenario the gasifier fuel input would be maximized producing a high calorific fuel during low load periods which can be stored or sold. In such a case the fuel feed to the “pyrolyser” would exceed the fuel feed to the boiler

With the investigations made in this project, it is a viable option to further investigate the installation of a gasifier onto the existing bark combustor with the suggested integration setup. The following conclusion can be drawn:

- Sufficient bed material can be transferred across a weir by means of directed extra fluidization to cover the heat demand of an 18 MW gasifier during low load operation of the BFB boiler
- Drying of the bark to 20% is recommended but even for bark with higher moisture a smaller sized gasifier can be realized with this concept.
- In a next step the effects on the boiler operation should be included into the considerations.

6 A1. Appendix

In Table 15 the particle size distribution in the experiments is shown. For calculating the mean particle size, it has been assumed that all particles in each tray has the size of its mean value. For example, it is assumed that all particles in tray 45-90 μm has a diameter of 67.5 μm. It is assumed that the mean diameter above 250 μm is 275 μm.

Table 15: Particle size distribution in the bed material used in the experiments

Tray span (μm)	Weight(g)	Mass fraction (w-%)
0-45	3.51	5.15
45-90	12.86	12.24
90-125	37.36	55.02
125-150	15.46	22.77
150-180	3.07	4.52
180-212	0.11	0.16
212-250	0.03	0.04
250<	0.06	0.09

7 References

[1] D. Athanassiadis T. Räisänen. Basic chemical composition of the biomass components of pine, spruce and birch. Technical report 1.2, Forest refine, 2013
[2] C. Gustavsson. *Added value from biomass by broader utilization of fuels and CHP plants.* PhD thesis, Karlstad University Studies, 2016
[3] A. Gandini, C. Pascoal Neto, A. J.D Silvestre. Suberin: A promising renewable resource for novel macromolecular materials. Progress in Polymer Science, 31(10):878-892, Oct 2006
[4] C. Breitholtz. The gasifier at Värö. *In IEA Technical Meeting*, 3-5 May 2009
[5] K. Salo. Biomass gasification in P&P industry. In *IEA Task 33 Meeting*, Andritz, Carbona Inc., Oct 2011
[6] Stanley E. Corder. Properties and usage of bark as an energy source. *Forest Research laboratory*, (31), Apr 1976.
[7] E. Alakangas. Properties of wood fuels used in Finland. BIOSOUTH project 2030, VTT, 2005.
[8] E. Kurkela. Thermal gasification for power and fuels. VTT-Gasification team, VTT research centre of Finland, Mar 2011
[9] F. Lind, M. Seemann, H. Thunman, A. Larsson, M. Israelsson. Using ilmenite to reduce the tar yield in a dual fluidized bed gasification system. Energy and Fuels, 28(4):2632-2644, Mar 2014. DOI: 10.1021/ef500132p
[10] Marinkovic, J., Thunman, H., Knutsson, P., & Seemann, M. (2015). Characteristics of olivine as a bed material in an indirect biomass gasifier. *Chemical Engineering Journal*, *279*, 555-566.
[11] T. Suda, Y. Matsuzawa, H. Tani, G. Xu, T. Muramaki. The superior technical choice for dual fluidized bed gasification. *Industrial and chemical engineering research*, 45(7):2281-2286, Feb 2006. DOI: 10.1021/ie051099r.
[12] T. Muramaki, K. Matsouka, K. Kuramoto and Y. Suzuki. Steam gasification of woody biomass in a circulating dual bubbling fluidized bed system. *Energy and fuels*, 22(3): 1980-1985, Mar 2008. DOI: 10.1021/ef700726s
[13] Zhao, K., Thunman, H., Pallarès, D., & Ström, H. (2017). Control of the solids retention time by multi-staging a fluidized bed reactor. *Fuel Processing Technology*, *167*, 171-182.
[14] P.C.A. Bergman, A. van der Drift, B.J. Vreugdenhil, C.M. van der Meijden, H.J. Veringa. Scale-up of the milena biomass gasification technology. In *17th european biomass conference and exhibition*, 2009.
[15] S. Weeks. Rialto renewable energy center-synthetic fuels and renewable electric power from biomass. In *NC: Biorefinery deployment collaborative*, 2009.
[16] H. Boerrigter et. Al. Gas cleaning for integrated biomass gasification (bg) and fischer-tropsch (ft) systems. Project Report 04-056, ECN Biomass, 2004.
[17] J-W. Könemann. Most efficient energy from waste technology. In *Gasification technology conference San Francisco*, number 2014 5.3 Royal Dahlman, GSTC, Oct 2014
[18] A. Larsson. Operational experience of the gobigas plant. In *Gasification summit*. GoBiGas, Göteborg Energi, Mar 2017.
[19] K. Bosch, C. Aichernig, H. Hofbauer, M. Bolhar-Nordenkampf, R. Rauch. Biomass chp plant güssing-using gasification for power generation. In *Int. Conference on biomass utilization*, 2002.
[20] H. Thunman, M. Seemann. The new chalmers research gasifier. In *ICPS 09*, 2009
[21] J. Brown. Biomass gasification: Fast internal circulating fluidised bed gasifier characterisation and comparison. Master's Thesis, university of Cantebury, 2006

[22] A. Moreno, A. Calbro, L. Leto, C. Dispenza. Simulation model of a molten carbonate fuel cells-microturbine hybrid system. *Applied thermal engineering*, 31(6-7):1263-1271, May 2011
[23] N.B. Rasmussen. Technologies relevant for gasification and methanation in Denmark. Project Report ForskNG 10689, Danish gas technology centre, 2012.
[24] T. Suda, T. Muramaki, L. Dong, G. Xu. Potential approaches to improve gasification of high water content biomass rich in cellulose in dual fluidized bed. *Fuel processing technology*, 91(8):882-888, Aug 2010
[25] J. Liu, C. Lu, S. Liu, C. Liu, L. Wei, S. Xu. A novel process of biomass gasification for hydrogen-rich gas with solid heat carrier: preliminary experimental results. *Energy and fuels*, 20(5):2266-2273, Aug 2006
[26] H. Boerrigter, A. van der Drift. Synthesis gas from biomass for fuels and chemicals. Report 06-001, ECN, 2006
[27] J. He, W. Zhang, K Göransson, U. Söderlind. Review of syngas production via biomass dfbgs. *Renewable and sustainable energy reviews*, 15(1):482-492, Jan 2011
[28] V. G. McDonell. Key issues associated with syngas and high-hydrogen fuels. Technical Report 3.1, Advanced Power and Energy Program, university of California, 2006
[29] S. Nordin, H. Larsson. Compact and efficient gas-ir dryer for drying of paper and board. Technical Report 263, SGC, Scheelegatan 3 malmö, 2013
[30] NIFES consulting group. Drying in the paper industry. Technical Report 287, European sommision, 8 woodside terrace, Glasgow, 1998
[31] J. Isaksson. Replacing Lime Kiln Fuel Oil with Gasified Biomass. In *Forum on Energy: Immediate Solutions, Emerging Technologies*, TAPPI, Kvaerner power OY, May 2006
[32] E. Kurkela. Thermal gasification for power and fuels. In *Business from Technology*. VTT, Technical research centre of Finland, Sep 2010
[33] J. Held. Gasification – status and technology. Technical Report 240, SGC, Scheelegatan 3 Malmö, 2012
[34] H. Boerrigter, et. al. Olga tar removal technology. Project report 05-009, ECN biomass, 1755 ZG Petten, The Netherlands, 2005
[35] M. Karlbrink. An evaluation of the performance of the gobigas gasification process. Master's Thesis, Chalmers University of Technology, Aug 2015
[36] D. Maggiola, M.Seemann, H. Thunman, O. Santos, A. Larsson, S. Sasic, H. Ström Functional surfaces for heat recovery during syngas production: can wettening lead to self-cleaning? (submitted)
[37] R. O. Blosser, H.S. Oglesby. Information on the sulfur content of bark and its contribution to SO_2 emissions when burned as a fuel, *Air pollution control association*, 30(7):769-772, Mar 2012. DOI: 10.1080/00022470.1980.10465107
[38] BillerudKorsnäs. Operational and environmental description. Pdf at webpage, 2013
[39] Ragbuhir Gupta. High-temperature sulfur removal in gasification applications. Center of Energy Technology, RTI international, Aug 2007
[40] M. Liberg Kristiansson, K. Andersson. Underlag för samråd enligt miljöbalken. Technical report, E.ON. gasification development, 2011
[41] A. Larsson. *Fuel conversion in a dual fluidized bed gasifier.* PhD thesis, Chalmers University of Technology, 2014
[42] L.R. Glicksman. Scaling relationships for fluidized beds. *Chemical Engineering Science*, 39(9):1373-1379, 1984
[43] B.M. Halvorsen, R.K. Thapa, C. Pfieifer. Scaling of biomass gasification reactor using cfd simulation. Technical Report, Department of Process Energy and Environmental Technology, Telemark University College, Norway, Sep 2013

[44] M.L. Sperb Indrusiak, F. Anderson Pedroso, F. Zinani. Numerical study if circulating fluidised beds built using glicksman's simplified and full sets of scaling parameters. *Brazilian Society of Mechanical Sciences and Engineering*, 38(7):2085-2096, Oct 2016. DOI: 0.1007/s40430-016-0502-1
[45] Octave Levenspiel, Daizo Kunii. *Fluidization Engineering 2nd Edition.* Chemical Engineering. Butterworth-Heinemann, 1991
[46] R. Shankar Subramanian. Flow through packed and fluidized beds. Technical report, Department of chemical and biomolecular engineering, Clarkson University, 2004. Retrieved from https://pdfs.semanticscholar.org/fcc9/c3b45f43b26ef70086353755a30e8a02a7bb.pdf

EVOLUTIONARY BIOMASS CONVERSION IN PULP AND PAPER INDUSTRIES

Förgasning av bark skulle kunna skapa ett energiflöde som gör pappersbruk oberoende av fossila bränslen. Energimarknaden är dock osäker. Framtida prissättning av utsläppsrättigheter för koldioxid, kemikalier och biobränslen är okänd, samtidigt som investeringar i anläggningar för förbränning och förgasning behöver vara långsiktiga för att täcka de höga kostnaderna.

Ett klokt val kan därför vara en indirekt påhängsförgasare som kan integreras med en befintlig fluidiserad bäddpanna av cirkulerande eller bubblande typ. Att använda gasen som bränngas är det minst kapitalintensiva och förgasaren kan kombineras med en gasrening för högre krav på renhet. Det innebär också att kopplingen till brukets övriga energiflöden är mjuk och kan utvecklas efter hand eftersom pannan fortsatt kan köras som vanligt, det vill säga utan förgasaren i drift, om det inte finns behov för exempelvis bränngas.

Här redovisas vilka gaskvalitéer man kan förvänta sig av olika restproduktsströmmar. Resultatet är intressant för ägare av massa- och pappersbruk eftersom de olika processkonfigurationer som föreslås visar potentialen för framtida utbyggnad.